HOCHSCHILD POLYTOPES

VINCENT PILAUD AND DARIA POLIAKOVA

ABSTRACT. The (m, n)-multiplihedron is a polytope whose faces correspond to m-painted n-trees, and whose oriented skeleton is the Hasse diagram of the rotation lattice on binary m-painted n-trees. Deleting certain inequalities from the facet description of the (m, n)-multiplihedron, we construct the (m, n)-Hochschild polytope whose faces correspond to m-lighted n-shades, and whose oriented skeleton is the Hasse diagram of the rotation lattice on unary m-lighted n-shades. Moreover, there is a natural shadow map from m-painted n-trees to m-lighted n-shades, which turns out to define a meet semilattice morphism of rotation lattices. In particular, when $m = 1$, our Hochschild polytope is a deformed permutahedron whose oriented skeleton is the Hasse diagram of the Hochschild lattice.
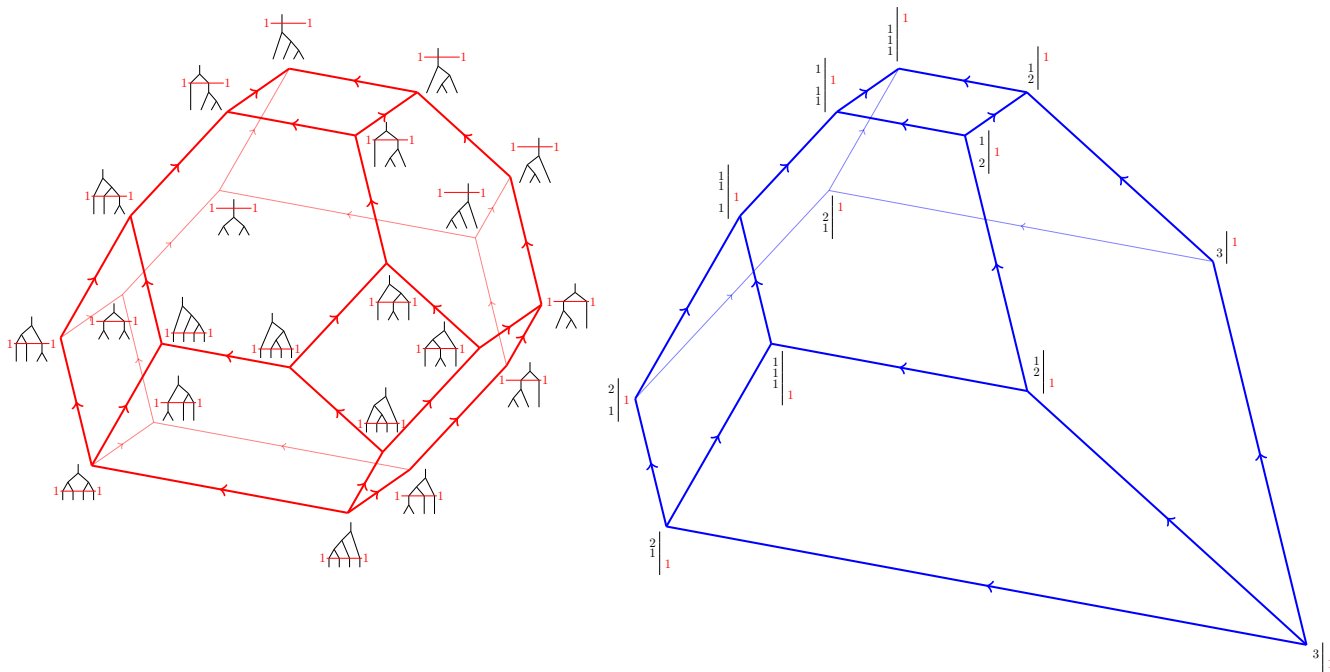
FIGURE 1. The multiplihedron $\mathbb{M}\mathrm{ul}(1, 3)$ (left) and the Hochschild polytope $\mathbb{H}\mathrm{och}(1, 3)$ (right).

CONTENTS

INTRODUCTION

We present a remake of the famous combinatorial, geometric, and algebraic interplay between permutations and binary trees. In the original story, the central character is the surjective map from permutations to binary trees (given by successive binary search tree insertions [Ton97, HNT05]). This map enables us to construct the Tamari lattice [Tam51] as a lattice quotient of the weak order [Rea06], the sylvester fan as a quotient fan of the braid fan [Rea05], Loday's associahedron [SS93, Lod04] as a removahedron of the permutahedron, and the Loday–Ronco Hopf algebra [LR98] as a Hopf subalgebra of the Malvenuto–Reutenauer Hopf algebra [MR95]. Many variations of this saga have been further investigated, notably for other lattice quotients of the weak order [Rea05, CP17, PP18, Pil18, PS19, Pil19] and for generalized associahedra arizing from finite type cluster algebras [FZ02, FZ03, Rea06, RS09, HLT11, HPS18]. See [PSZ23] for a recent survey on this topic.

In the present remake, permutations are replaced by binary m-painted n-trees (binary trees with n nodes with m horizontal labeled edge cuts), while binary trees are replaced by unary m-lighted n-shades (partitions of n with m labels inside its gaps). While their precise definitions are delayed to Section 1, these combinatorial objects are already illustrated in Figure 1 for $m = 1$ and $n = 3$. The m-painted n-trees already appeared in [CP22, Sect. 3.1], inspired from the case $m = 1$ studied in [Sta63, SU04, For08, FLS10, MW10, AD13]. They are mixtures between the permutations of $[m]$ and the binary trees with n nodes (here, mixture is meant in the precise sense of shuffle [CP22], which is very different from other interpolations of permutations and binary trees, notably permutrees [PP18]). The m-lighted n-shades are introduced in this paper, inspired from the case $m = 1$ studied in [ACD11, Pol20, Cha20, Com21, Müh22]. Here again, the central character is a natural surjective map from the former to the latter. Namely, the shadow map sends an m-painted n-tree to the m-lighted n-shade obtained by collecting the arity sequence along the right branch. In other words, this map records the shadow projected on the right of the tree when the sun sets on the left of the tree.

We first use this map for lattice purposes. It was proved in [CP22] that the right rotation digraph on binary m-painted n-trees (a mixture of the simple transposition digraph on permutations and the right rotation digraph on binary trees) defines a lattice. We consider here the right rotation digraph on unary m-lighted n-shades. In contrast to the rotation graph on binary m-painted n-trees, the rotation graph on unary m-lighted n-shades is regular (each node has $m + n - 1$ incoming plus outgoing neighbors). We prove that it defines as well a lattice by showing that the shadow map is a meet semilattice morphism (but not a lattice morphism). When $m = 0$, this gives an unusual meet semilattice morphism from the Tamari lattice to the boolean lattice (distinct from the usual lattice morphism given by the canopy map). When $m = 1$, this gives a connection, reminiscent of [Pol20], between the painted tree rotation lattice and the Hochschild lattice introduced in [Cha20] and studied in [Com21, Müh22]. The Hochschild lattice has nice lattice properties: it was proved to be congruence uniform and extremal in [Com21], its Galois graph, its canonical join complex and its core label order were described in [Müh22], and its Coxeter polynomial was conjectured to be a product of cyclotomic polynomials [Com21, Appendix]. For $m > 1$, computational experiments indicate that the m-lighted n-shade rotation lattice is still constructible by interval doubling (hence semi-distributive and congruence uniform), but it is not extremal and its Coxeter polynomial is not a product of cyclotomic polynomials. However, its subposet induced by unary m-lighted n-shades where the labels of the lights are ordered seems to enjoy all these nice properties. The lattice theory of the m-lighted n-shade right rotations certainly deserves to be investigated further.

We then use the shadow map for polytopal purposes. It was proved in [CP22] that the refinement poset on all m-painted n-trees is isomorphic to the face of a polytope, called the (m, n)-multiplihedron $\mathbb{Mul}(m, n)$. This polytope is a deformed permutahedron (a.k.a. polymatroid [Edm70], or generalized permutahedron [Pos09, PRW08]) obtained as the shuffle product [CP22] of an m-permutahedron with an n-associahedron of J.-L. Loday [SS93, Lod04]. Oriented in a suitable direction, the skeleton of the (m, n)-multiplihedron is isomorphic to the right

rotation digraph on binary m-painted n-trees [CP22]. Similarly, we show here that the refinement poset on all m-lighted n-shades is isomorphic to the face lattice of a polytope, called the (m, n)-Hochschild polytope $\mathbb{Hoch}(m, n)$. We obtain this polytope by deleting some inequalities in the facet description of the (m, n)-multiplihedron. We also work out the vertex description of the (m, n)-Hochschild polytope and its decomposition as Minkowski sum of faces of the standard simplex. We obtain a deformed permutahedron whose oriented skeleton is isomorphic to the right rotation digraph on unary m-lighted n-shades. When $m = 0$, the $(0, n)$-multiplihedron is the n-associahedron and the $(0, n)$-Hochschild polytope is a skew cube (which is not a parallelotope). When $m = 1$, the $(1, n)$-multiplihedron is the classical multiplihedron introduced and studied in [Sta63, SU04, For08, FLS10, MW10, AD13], and the $(1, n)$-Hochschild polytope is a deformed permutahedron realizing the Hochschild lattice. Let us insist here on the fact that our Hochschild polytope provides a much stronger geometric realization of the Hochschild lattice than the already two existing ones. Namely, the Hochschild lattice is known to be realized

- on the one hand, as the standard orientation of a graph drawn on the boundary of an hypercube (see Section 3), but this graph is not the skeleton of a convex polytope,
- on the other hand, as an orientation of the skeleton of a convex polytope called freehedron and obtained as a truncation of the standard simplex [San09] (or equivalently as the Minkowski sum of the faces of the standard simplex corresponding to all initial and final intervals), but this orientation cannot be obtained as a Morse orientation given by a linear functional (see Example 63).

Finding a deformed permutahedron whose skeleton oriented in the standard linear direction is isomorphic to the Hasse diagram of the Hochschild lattice was an open question raised by F. Chapoton.

The groupies of the permutahedron–associahedron saga probably wonder about properties of the singletons of the shadow map (*i.e.* a unary m-lighted n-shade whose shadow fiber consists of a single binary m-painted n-tree). Interestingly, these singletons are counted by binomial transforms of Fibonacci numbers. Moreover, the common facet defining inequalities of $\mathbb{Mul}(m, n)$ and $\mathbb{Hoch}(m, n)$ are precisely those that contain a common vertex of $\mathbb{Mul}(m, n)$ and $\mathbb{Hoch}(m, n)$. This property was essential in the original realization of the Cambrian fans of [RS09] as generalized associahedra [HLT11].

Somewhat independently, we also show that the right rotation digraph on unary m-lighted n-shades can also be realized on the boundary of an hypercube, generalizing the existing cubic coordinates for the Hochschild lattice [Com21]. Cubic coordinates are well known for many famous lattices (they are called Lehmer codes for weak Bruhat lattices, and bracket vectors for Tamari lattices). In [SU04] a stronger notion of cubic subdivisions was used to construct combinatorial diagonals for the corresponding polytopes. When available, cubic coordinates also provide an elegant alternative proof of the lattice property.

We conclude this introduction by a glance at the algebraic motivation for painted trees and lighted shades, coming from homological algebra. The family of multiplihedra controls the notion of A_∞-morphisms. If A and B are two A_∞-algebras and $f : A \to B$ is an A_∞-morphism, then each face of the multiplihedron encodes an operation $A^{\otimes n} \to B$, with the cellular differential taking care of the relations. Equivalently, one can view the faces of the multiplihedron as encoding the operations $A^{\otimes n-1} \otimes M \to N$, where A is an A_∞-algebra and M and N are A_∞-modules over A. Now if one assumes A strictly associative (DG instead of A_∞), there are clearly less such operations. A universal basis for such operations was constructed in [ACD11, Thm. 6.4] in the form of short forest-tree-forest triples, and it was observed in [Pol20, Sect. 5] that these items are nothing else but the faces of the freehedra of [San09]. This gave the case $m = 1$ of the shadow map [Pol20, Construction 2].

The paper is organized as follows. In Section 1, we survey the m-painted n-trees from [CP22] and introduce the m-lighted n-shades, and we consider the shadow map sending the former to the latter. In Section 2, we recall the descriptions of the (m, n)-multiplihedron, realizing the m-painted n-tree refinement lattice, from which we derive the construction of the (m, n)-Hochschild polytope, realizing the m-lighted n-shade refinement lattice. Finally, we discuss in Section 3 the cubic coordinates for m-painted n-trees and m-lighted n-shades.

1. PAINTED TREES AND LIGHTED SHADES

In this section, we first recall the combinatorics of m-painted n-trees (Section 1.1) and introduce that of m-lighted n-shades (Section 1.2). We then analyse the natural shadow map from m-painted n-trees to m-lighted n-shades (Section 1.3), with a particular focus on its singletons (Section 1.4).

1.1. m-**painted n-trees.** We start with the combinatorics of m-painted n-trees already studied in details in [CP22, Sect. 3.1]. It was inspired from the case $m = 1$ studied in [Sta63, SU04, For08, FLS10, MW10, AD13].

Definition 1. An *n-tree* is a rooted plane tree with $n + 1$ leaves.

As usual, we orient such a tree towards its root and label its vertices in inorder. Namely, each node of degree ℓ is labeled by an $(\ell - 1)$-subset $\{x_1, \ldots, x_{\ell-1}\}$ such that all labels in its ith subtree are larger than x_{i-1} and smaller than x_i (where by convention $x_0 = 0$ and $x_\ell = n + 1$). Note in particular that unary nodes receive an empty label.

Definition 2 ([CP22, Def. 104]). A *cut* of an n-tree T is a subset c of nodes of T containing precisely one node along the path from the root to any leaf of T. A cut c is *below* a cut c' if the unique node of c is after the unique node of c' along any path from the root to a leaf of T (note that we draw trees growing downward).

Definition 3 ([CP22, Def. 105]). An *m-painted n-tree* $\mathbb{T} := (T, C, \mu)$ is an n-tree C together with a sequence $C := (c_1, \ldots, c_k)$ of k cuts of T and an ordered partition μ of $[m]$ into k parts for some $k \in [m]$, such that

  - c_i is below c_{i+1} for all $i \in [k-1]$,
  - $\bigcup C := c_1 \cup \cdots \cup c_k$ contains all unary nodes of T.

We represent an m-painted n-tree $\mathbb{T} := (T, C, \mu)$ as a downward growing tree T, where the cuts of C are red horizontal lines, labeled by the corresponding parts of μ. As there is no ambiguity, we write 12 for the set $\{1, 2\}$. See Figures 2, 4 and 5 for illustrations.

We now associate to each m-painted n-tree a preposet (*i.e.* a reflexive and transitive binary relation) on $[m + n]$. These preposets will be helpful in several places.

Definition 4. Consider an m-painted n-tree $\mathbb{T} := (T, C, \mu)$. Orient T towards its root, label each node x of T by the union of the part in μ corresponding to the cut of C passing through x (empty set if x is in no cut of C) and the inorder label of x in the tree T shifted by m, and finally merge together all nodes contained in each cut. We then define $\preccurlyeq_{\mathbb{T}}$ as the preposet on $[m + n]$ where $i \preccurlyeq_{\mathbb{T}} j$ if there is a (possibly empty) oriented path from the node containing i to the node containing j in the resulting oriented graph. See Figure 3.

We now use these preposets to define the refinement poset on m-painted n-trees.

Definition 5 ([CP22, Def. 108]). The *m-painted n-tree refinement poset* is the poset on m-painted n-trees ordered by refinement of their corresponding preposets, that is, $\mathbb{T} \leq \mathbb{T}'$ if $\preccurlyeq_{\mathbb{T}} \supseteq \preccurlyeq_{\mathbb{T}'}$.

Remark 6. Alternatively [CP22, Prop. 111], we could describe the cover relations of the m-painted n-tree refinement poset combinatorially by three types of operations, as was done in [CP22, Def. 106] and illustrated in Figure 4. Namely, to obtain the elements covered by an m-painted n-tree, one can

  (i) contract an edge whose child is contained in no cut,
  (ii) contract all edges from a parent in no cut to its children all in the same cut,
  (iii) join together two consecutive cuts with no node in between them.

In the following statement, we denote by $|T|$ the number of nodes of a tree T (including unary nodes), and define $|C| := k$ and $|\bigcup C| := |c_1 \cup \cdots \cup c_k|$ for $C = (c_1, \ldots, c_k)$.

Proposition 7 ([CP22, Props. 107 & 116]). *The m-painted n-tree refinement poset is a meet semi-lattice ranked by* $m + n - |T| - |C| + |\bigcup C|$.

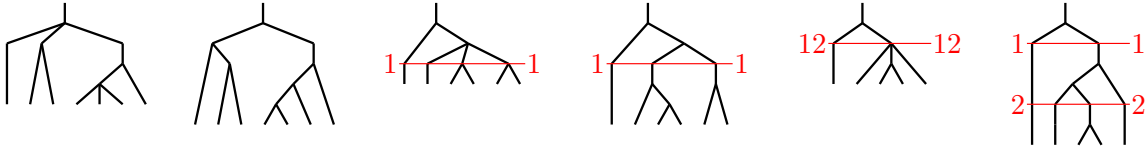We now define another lattice structure, but on minimal m-painted n-trees. See Figures 6 to 8.
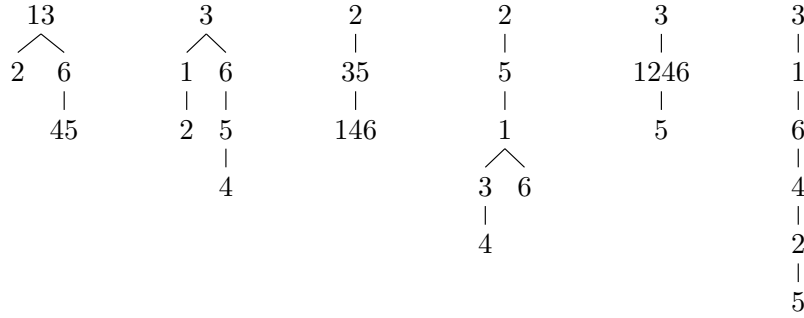
FIGURE 2. Some m-painted n-trees with $m + n = 6$.

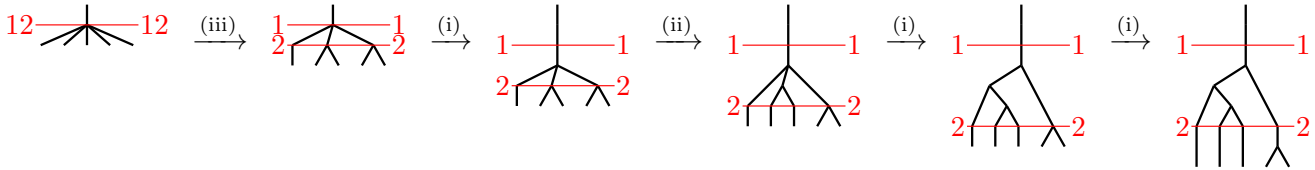FIGURE 3. The preposets $\preccurlyeq_{\mathbb{T}}$ associated to the m-painted n-trees $\mathbb{T}$ of Figure 2.

FIGURE 4. Refinements of some 2-painted 4-trees. Each refinement is labeled by its type.

Definition 8 ([CP22, Def. 112])**.** An m-painted n-tree $\mathbb{T} := (T, C, \mu)$ is *binary* if it has rank 0, meaning that all nodes in $\bigcup C$ are unary, while all nodes not in $\bigcup C$ are binary. The *binary m-painted n-tree right rotation digraph* is the directed graph on binary m-painted n-tree with an edge $(\mathbb{T}, \mathbb{T}')$ if and only if there exists $1 \le i < j \le m + n$ such that $\preccurlyeq_{\mathbb{T}} \smallsetminus \{(i, j)\} = \preccurlyeq_{\mathbb{T}'} \smallsetminus \{(j, i)\}$.

Remark 9. Again, we could alternatively describe the right rotations on binary m-painted n-trees combinatorially by three types of operations, as was done in [CP22, Def. 112] and illustrated in Figure 5. Namely, the cover relations correspond to

  (i) right rotate an edge joining two binary nodes,
 (ii) sweep a binary node by a cut below it,
(iii) exchange the labels of two consecutive cuts with no node in between them, passing the small label above the large label.

Proposition 10 ([CP22, Def. 119])**.** *The binary m-painted n-tree right rotation digraph is the Hasse diagram of a lattice.*

Example 11. When $m = 0$, the 0-painted n-tree rotation lattice is the Tamari lattice [Tam51, HT72]. When $m = 1$, the 1-painted n-tree rotation lattice is the multiplihedron lattice introduced in [CP22].

Remark 12. Note that the m-painted n-tree rotation lattice is meet semidistributive, but not join semidistributive when $m \ge 1$.

We conclude this recollection on m-painted n-trees by some enumerative observations. See also Tables 1, 2 and 3 in Appendix A.1.
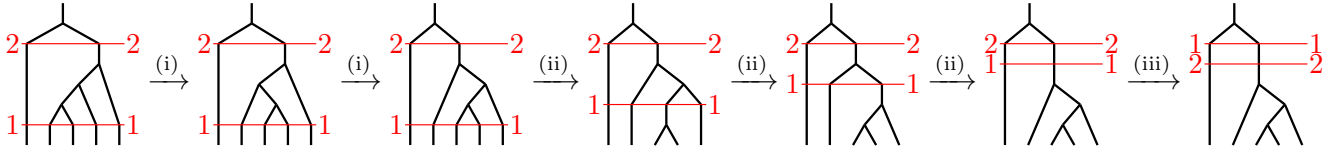
FIGURE 5. Rotations of some binary 2-painted 4-trees. Each rotation is labeled by its type.
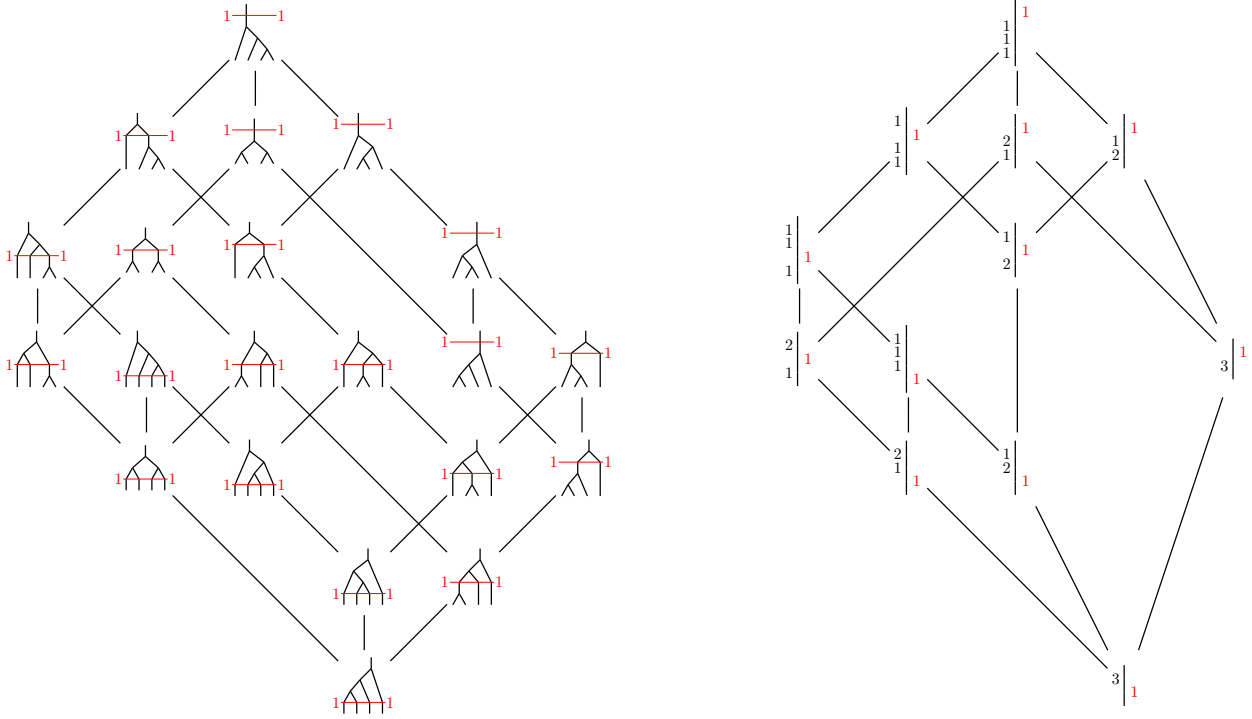
FIGURE 6. The 1-painted 3-tree (left) and 1-lighted 3-shade (right) rotation lattices.

Proposition 13 ([CP22, Prop. 126]). *The number of binary m-painted n-trees is*

$$m! \, [y^{n+1}] \, \mathcal{C}^{(m+1)}(y),$$

where $[y^{n+1}]$ selects the coefficient of y^{n+1}, and $\mathcal{C}^{(i)}(y)$ is defined for $i \geq 1$ by

$$\mathcal{C}^{(1)}(y) := \mathcal{C}(y) \qquad and \qquad \mathcal{C}^{(i+1)}(y) := \mathcal{C}\big(\mathcal{C}^{(i)}(y)\big),$$

where

$$\mathcal{C}(y) = \frac{1 - \sqrt{1 - 4y}}{2}$$

is the Catalan generating function. See Table 1 in Appendix A.1 for the first few numbers.

Proposition 14 ([CP22, Prop. 127]). *The number of rank $m + n - 2$ m-painted n-trees is*

$$\binom{n+1}{2} - 1 + 2^{m+n} - 2^n.$$

See Table 2 in Appendix A.1 for the first few numbers.

Proposition 15 ([CP22, Prop. 128])**.** *The generating function $\mathcal{PT}(x, y, z) := \sum\limits_{m,n,p} PT(m, n, p)\, x^m y^n z^p$ of the number of rank p m-painted n-trees is given by*

$$\mathcal{PT}(x, y, z) = \sum_m x^m \sum_{k=0}^{m} \mathcal{S}\big(\mathcal{S}_*^{(k)}(y, z), z\big)\, \mathsf{S}(m, k)\, z^{m-k},$$

where $\mathsf{S}(m, k)$ is the number of surjections from $[m]$ to $[k]$,

$$\mathcal{S}(y, z) = \frac{1 + yz - \sqrt{1 - 4y - 2yz + y^2 z^2}}{2(z + 1)}$$

is the Schröder generating function, and $\mathcal{S}_*^{(i)}(y, z)$ is defined for $i \geq 0$ by

$$\mathcal{S}_*^{(0)}(y, z) := y, \quad \mathcal{S}_*^{(1)}(y, z) := (1 + z)\,\mathcal{S}(y, z) - yz \quad \text{and} \quad \mathcal{S}_*^{(i+1)}(y, z) := \mathcal{S}_*^{(i)}\big(\mathcal{S}_*^{(1)}(y, z), z\big).$$

See Table 3 in Appendix A.1 for the first few numbers.

Example 16. When $m = 0$, the number of 0-painted n-trees of rank 0, rank $n - 2$ and arbitrary rank are respectively given by the classical Catalan numbers (A000108), the interval numbers (A000096) and the Schröder numbers (A001003).

1.2. m-**lighted n-shades.** We now introduce the main new characters of this paper, which will later appear as certain shadows of m-painted n-trees.

Definition 17. An *n-shade* is a sequence of (possibly empty) tuples of integers, whose total sum is n. An *m-lighted n-shade* $\mathbb{S} := (S, C, \mu)$ is an n-shade S together with a set C of k distinguished positions in S, containing all positions of empty tuples of S, and an ordered partition μ of $[m]$ into k parts for some $k \in [m]$.

Remark 18. Alternatively, we could define an m-lighted n-shade as a pair (S, C) of sequences of the same length, where S contains (possibly empty) tuples of integers and has total sum n, while C contains (possibly empty) subsets of $[m]$ whose union is $[m]$, and c_i is nonempty when s_i is the empty tuple. We preferred the version of Definition 17 to be more parallel to Definition 3.

We represent an m-lighted n-shade $\mathbb{S} := (S, C, \mu)$ as a vertical line, with the tuples of the sequence S in black on the left, and the cuts of C in red on the right. As there is no ambiguity, we write 12 for the tuple $(1, 2)$ or the set $\{1, 2\}$. See Figures 9, 11 and 12 for illustrations.

We now associate to each m-lighted n-shade a preposet on $[m + n]$. These preposets will be helpful in several places.

Definition 19. Consider an m-lighted n-shade $\mathbb{S} := (S, C, \mu)$. The *preceeding sum* $ps(x)$ of an entry x in a tuple of S is m plus the sum of all entries that appear weakly before x in S (meaning either the entries in a strictly earlier tuple of S, or the weakly earlier entries in the same tuple as x). We then define $\preccurlyeq_{\mathbb{S}}$ as the preposet on $[m + n]$ given by the relations

- $i \preccurlyeq_{\mathbb{S}} j$ if $i, j \in [m]$ and i appears weakly after j in μ,
- $k \preccurlyeq_{\mathbb{S}} ps(y)$ if x and y are elements of tuples of S such that the tuple of x appears weakly after the tuple of y, and $ps(x) - x < k \leq ps(x)$,
- $i \preccurlyeq_{\mathbb{S}} ps(x)$ if $i \in [m]$ and x is an element of a tuple of S which appears weakly before the cut containing i,
- $k \preccurlyeq_{\mathbb{S}} i$ if $i \in [m]$ and $ps(x) - x < k \leq ps(x)$ for some element x of a tuple of S which appears weakly after the cut containing i.

See Figure 10.

Remark 20. Define the Hasse diagram of a preposet $\preccurlyeq$ on X to be the Hasse diagram of the poset $\preccurlyeq/\equiv$ on the classes of the equivalence relation $\equiv := \{(x, y) \in X \times X \mid x \preccurlyeq y \text{ and } y \preccurlyeq x\}$ defined by $\preccurlyeq$. In contrast to the preposet $\preccurlyeq_{\mathbb{T}}$ of an m-painted n-tree $\mathbb{T}$, note that by definition the Hasse diagram of the preposet $\preccurlyeq_{\mathbb{S}}$ of an m-lighted n-shade $\mathbb{S}$ is always a forest. More precisely, the Hasse diagram of $\preccurlyeq_{\mathbb{S}}$ is a caterpillar forest, whose path contains one node $\{ps(x_1), \ldots, ps(x_k)\}$ for each tuple $(x_1, \ldots, x_k)$ of $\mathbb{S}$.
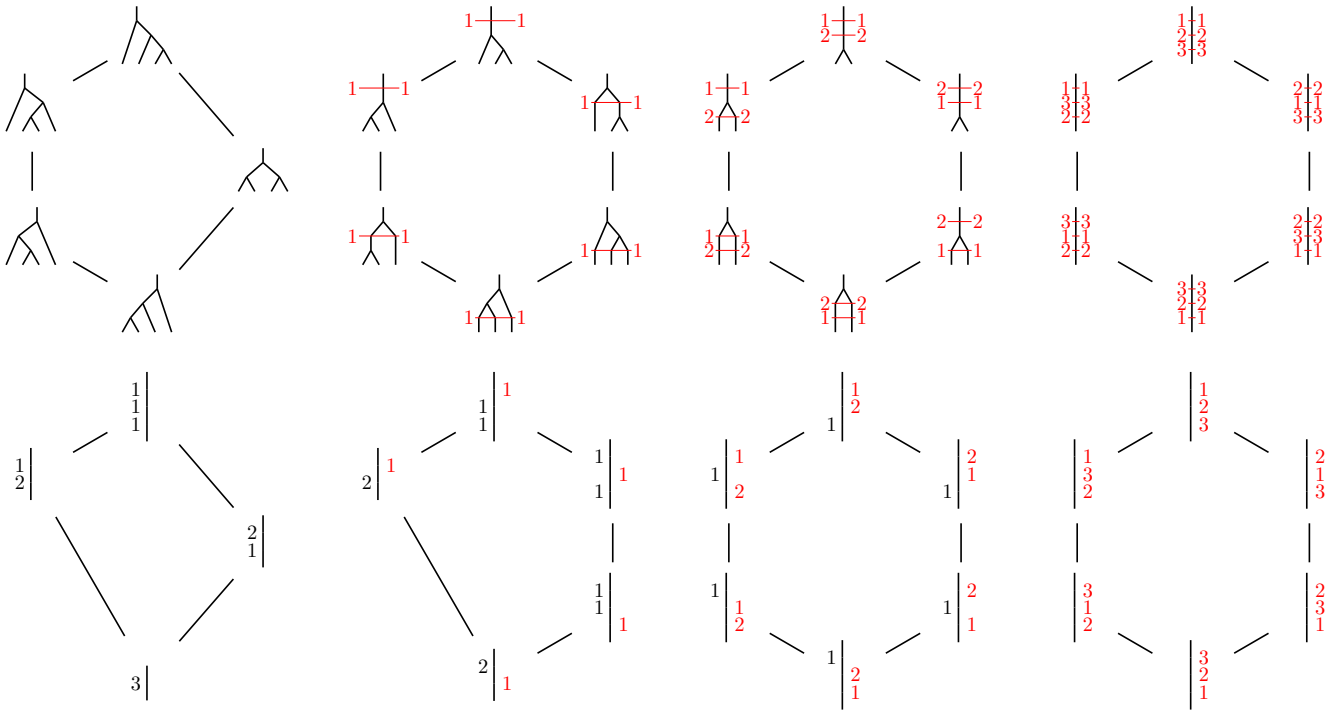
FIGURE 7. The m-painted n-tree rotation lattice (top) and the m-lighted n-shade rotation lattice (bottom) for $(m, n) = (0, 3)$, $(1, 2)$, $(2, 1)$, and $(3, 0)$ (left to right).
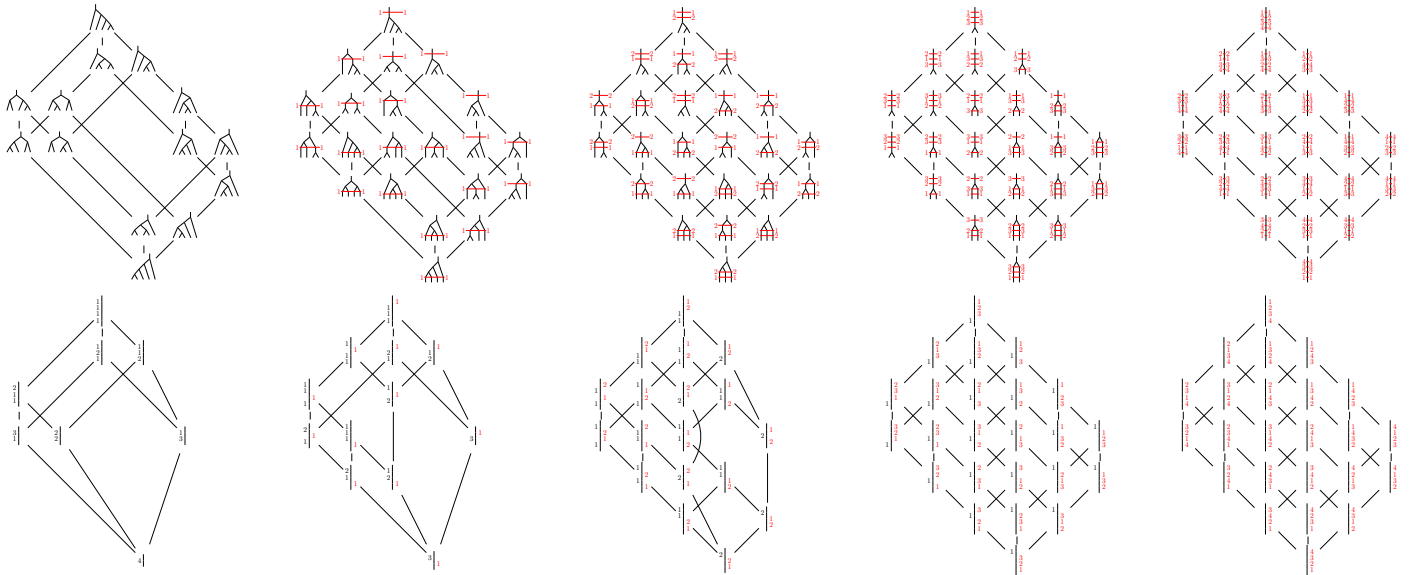

FIGURE 8. The m-painted n-tree rotation lattice (top) and the m-lighted n-shade rotation lattice (bottom) for $(m, n) = (0, 4)$, $(1, 3)$, $(2, 2)$, $(3, 1)$, and $(4, 0)$ (left to right).
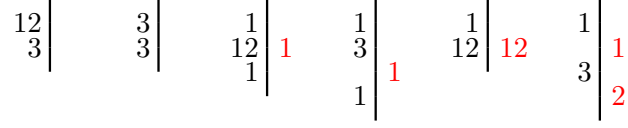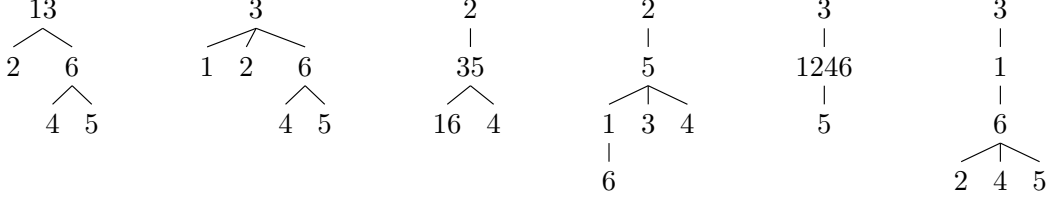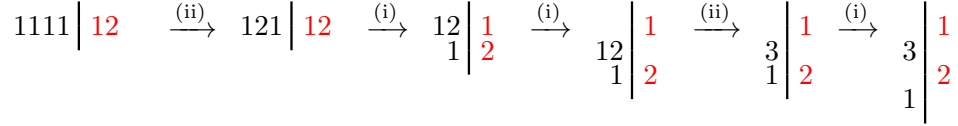
FIGURE 9. Some m-lighted n-shades with $m + n = 6$.

FIGURE 10. The preposets $\preccurlyeq_{\mathbb{S}}$ associated to the m-lighted n-shades $\mathbb{S}$ of Figure 9.

FIGURE 11. Refinements of some 2-lighted 4-shades. Each refinement is labeled by its type.

We now use these preposets to define the refinement poset on m-lighted n-shades.

Definition 21. The *m-lighted n-shade refinement poset* is the poset on m-lighted n-shades defined by refinement of their corresponding preposets, that is, $\mathbb{S} \leq \mathbb{S}'$ if $\preccurlyeq_{\mathbb{S}} \supseteq \preccurlyeq_{\mathbb{S}'}$.

Remark 22. Alternatively, we could describe the cover relations of the m-lighted n-shades refinement poset combinatorially by two types of operations, as illustrated in Figure 11. Namely, to obtain the elements covered by an m-lighted n-shade, one can

  (i) concatenate two consecutive (possibly empty) tuples, and merge their (possibly empty) cuts,
 (ii) replace one of the integers x inside a tuple by two integers y, z with $x = y + z$ and $y \geq 1$ and $z \geq 1$.

For a sequence $S := (s_1, \ldots, s_\ell)$ of tuples, we define $|S| := \ell$ and $\|S\| := \sum_{i \in [\ell]} |s_i|$, where $|s_i|$ is the length of the tuple s_i.

Proposition 23. *The m-lighted n-shade refinement poset is a meet semilattice ranked by $m - |S| + \|S\|$.*

Proof. For the rank, if $\mathbb{S} := (S, C, \mu)$ and $\mathbb{S}' := (S', C', \mu')$ are obtained by one of the two operations of Remark 22, then we have

  (i) $|S'| = |S| - 1$ and $\|S'\| = \|S\|$ when we concatenate two consecutive tuples,
 (ii) $|S'| = |S|$ and $\|S'\| = \|S\| + 1$ when we refine an integer into two inside one of the tuples.

In both situations, we get $\operatorname{rank}(\mathbb{S}') = \operatorname{rank}(\mathbb{S}) + 1$. Finally, the meet semilattice property will follow from Proposition 64. $\square$

We now define another lattice structure, but on minimal m-lighted n-shades. See Figures 6 to 8.

Definition 24. An m-lighted n-shade $\mathbb{S} := (S, C, \mu)$ is *unary* if it has rank 0, meaning that all tuples in $\bigcup C$ are empty tuples, while all tuples not in $\bigcup C$ are singletons. The *unary m-lighted n-shade right rotation digraph* is the directed graph on unary m-lighted n-shades with an edge $(\mathbb{S}, \mathbb{S}')$ if and only if there exists $1 \leq i < j \leq m + n$ such that $\preccurlyeq_{\mathbb{T}} \smallsetminus \{(i, j)\} = \preccurlyeq_{\mathbb{T}'} \smallsetminus \{(j, i)\}$.

$$\begin{array}{c}1\\ \hline 2\\ 3\ \ \ 1\end{array} \quad \xrightarrow{\ (i)\ } \quad \begin{array}{c}1\\ \hline 2\\ 1\\ \hline 2\\ 1\end{array} \quad \xrightarrow{\ (ii)\ } \quad \begin{array}{c}1\\ \hline 2\\ 1\\ \hline 2\end{array} \quad \xrightarrow{\ (ii)\ } \quad \begin{array}{c}1\\ \hline 2\\ 1\\ \hline 2\end{array} \quad \xrightarrow{\ (iii)\ } \quad \begin{array}{c}1\\ \hline 1\\ 2\\ \hline 1\\ 2\end{array}$$
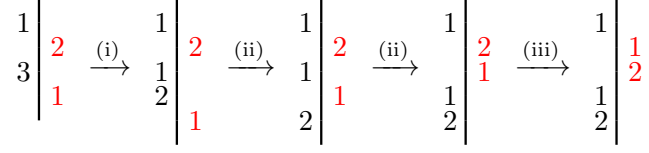
FIGURE 12. Rotations of some unary 2-lighted 4-shades. Each rotation is labeled by its type.

Remark 25. Again, we could alternatively describe the right rotations on unary m-lighted n-shades combinatorially by three types of operations, as illustrated in Figure 12. Namely, the cover relations correspond to

(i) replace a singleton (r) by two singletons $(s), (t)$ with $r = s + t$ and $s \geq 1$ and $t \geq 1$,
(ii) exchange a singleton with a cut below it,
(iii) exchange the labels of two consecutive cuts with no singleton in between them, passing the small label above the large label.

Remark 26. From Remark 25, we observe that any unary m-lighted n-shade $\mathbb{S}$ with singleton tuples $s_1, \ldots, s_k$ admits $m + k - 1 + \sum_{i \in [k]} (s_i - 1) = m + n - 1$ (left or right) rotations. In other words, the (undirected) rotation graph is regular of degree $m + n - 1$. Note that this can also be seen as a consequence of Remark 20.

The next statement will follow from Proposition 37.

Proposition 27. *The unary m-lighted n-shade right rotation digraph is the Hasse diagram of a lattice.*

Example 28. When $m = 0$, the 0-lighted n-shade rotation lattice is the boolean lattice. When $m = 1$, the 1-lighted n-shade rotation lattice is the Hochschild lattice studied in [Cha20, Com21, Müh22].

Remark 29. Computational experiments indicate that the m-lighted n-shade rotation lattice is constructible by interval doubling (hence semidistributive and congruence uniform). However, in contrast to the case when $m \leq 1$, it is not extremal (see [Müh22] for context), and its Coxeter polynomial is not a product of cyclotomic polynomials (see [Cha23] and [Com21, Appendix] for context). Nevertheless, its subposet induced by unary m-lighted n-shades where the labels of the lights are ordered (see also Definition 75) seems to enjoy all these nice properties. The lattice properties of the m-lighted n-shade rotation lattice and its subposet deserve to be investigated further.

We conclude this section on m-lighted n-shades by some enumerative observations. See also Tables 4, 5 and 6 in Appendix A.2.

Proposition 30. *The number of unary m-lighted n-shades is*

$$m! \sum_{\ell=1}^{n} \binom{m+\ell}{m} \binom{n-1}{\ell-1}.$$

See Table 4 in Appendix A.2 for the first few numbers.

Proof. The number of unary m-lighted n-shades with ℓ singletons is given by $m! \binom{m+\ell}{\ell} \binom{n-1}{\ell-1}$. Namely, choose the order of the cuts (hence $m!$ choices), the position of the m cuts and ℓ singletons (hence $\binom{m+\ell}{\ell}$ choices), and the values of the ℓ singletons (hence $\binom{n-1}{\ell-1}$ choices). $\square$

Proposition 31. *The number of rank $m + n - 2$ m-lighted n-shades is*

$$(2^m + 1)(n + 1) - 4 + \delta_{n=0}.$$

See Table 5 in Appendix A.2 for the first few numbers.

Proof. Consider an m-lighted n-shade $\mathbb{S} := (S, C, \mu)$ with $S := (s_1, \ldots, s_\ell)$ According to Proposition 23, $\mathbb{S}$ has rank $m + n - 2$ if and only if $n - 2 = \|S\| - |S| = \sum_{i \in [\ell]} |s_i| - 1$, or equivalently if and only if one of the following holds:

- either $\ell = 1$ and $s_1 = 1^{i-1} 2 1^{n-1-i}$ for some $i \in [n-1]$ (hence $n-1$ choices),
- or $\ell = 2$ and $s_1 = 1^i$ while $s_2 = 1^{n-i}$ for some $i \in [n-1]$ and the m labels are allocated arbitrarily on the two positions (hence $2^m(n-1)$ choices),
- or $\ell = 2$ and $s_1 = \varnothing$ while $s_2 = 1^n$ and the m labels are allocated on the two tuples, with at least one label on the first tuple (hence $2^m - 1$ choices),
- or $\ell = 2$ and $s_1 = 1^n$ while $s_2 = \varnothing$ and the m labels are allocated on the two tuples, with at least one label on the second tuple (hence $2^m - 1$ choices).

We obtain that there are $n - 1 + 2^m(n-1) + 2(2^m - 1) = (2^m + 1)(n + 1) - 4$ rank $m + n - 2$ m-lighted n-shades. The correction $\delta_{n=0}$ comes from the fact that the last three situations overlap when $n = 0$. $\qquad\square$

Proposition 32. *The generating function $\mathcal{LS}(x, y, z) := \sum\limits_{m,n,p} LS(m, n, p) \, x^m y^n z^p$ of the number of rank p m-lighted n-shades is given by*

$$\mathcal{LS}(x, y, z) = \sum_m x^m \sum_{k=0}^m \frac{(1-y)^k (1 - y(z+1))}{(1 - y(z+2))^{k+1}} \, \mathsf{S}(m, k) \, z^{m-k},$$

where $\mathsf{S}(m, k)$ is the number of surjections from $[m]$ to $[k]$. See Table 6 in Appendix A.2 for the first few numbers.

Proof. Denote by

$$\tau^\geq(y, z) = \frac{1}{1 - yz/(1-y)} = \frac{1-y}{1 - y(z+1)} \qquad \left(\text{resp.} \quad \tau^>(y, z) = \frac{y}{1 - y(z+1)} \right)$$

the generating function of all (resp. nonempty) tuples of integers, where y counts the sum, and z counts the length. For fixed integers $0 \leq k \leq m$, we claim that the generating function $\sum_{n,p} LS(m, n, p) \, y^n z^p$ of rank p m-lighted n-shades with k cuts is given by

$$\tau^\geq(x, y)^k \left(\frac{1}{1 - \tau^>(x, y)} \right)^{k+1} \mathsf{S}(m, k) \, z^{m-k} = \frac{(1-y)^k (1 - y(z+1))}{(1 - y(z+2))^{k+1}} \, \mathsf{S}(m, k) \, z^{m-k}$$

Indeed, to construct a rank p m-lighted shade with k cuts, we need to choose

- k possibly empty tuples for the cuts, hence k factors $\tau^\geq(x, y)$,
- $k + 1$ possibly empty sequences of nonempty tuples inbetween the cuts (including before the first cut and after the last cut), hence $k+1$ factors $\frac{1}{1 - \tau^>(x,y)}$,
- an ordered partition of $[m]$ into k parts, hence a factor $\mathsf{S}(m, k)$. $\qquad\square$

Example 33. When $m = 0$, the number of 0-painted n-trees of rank 0, rank $n-2$ and arbitrary rank are respectively given by 2^{n-1} (A000079), $2(n-1)$ (A005843) and 3^{n-1} (A000244). When $m = 1$, the number of 1-painted n-trees of rank 0, rank $n-1$ are respectively given by $2^{n-2}(n+3)$ (A045623) and $3n - 1$ (A016789).

1.3. Shadow map. We now describe a natural shadow map sending an m-painted n-tree to an m-lighted n-shade. Intuitively, the shadow is what you see on the right of the tree when the sun sets on its left. For instance, the m-painted n-trees of Figure 2 are sent to the m-lighted n-shade of Figure 9. We call *right branch* of a tree T the path from the root to the rightmost leaf of T.

Definition 34. The *shadow* of an n-tree T is the n-shade $\mathrm{Sh}(T)$ obtained by

- contracting all edges joining a child to a parent which does not lie on the right branch of T,
- replacing each node on the left branch of T by the tuple of the arities of its children except its rightmost.

The *shadow* of a cut c in T is the position $\mathrm{Sh}(c)$ in $\mathrm{Sh}(T)$ of the unique node of the right branch of T contained in c. For a sequence $C = (c_1, \ldots, c_k)$, define $\mathrm{Sh}(C) := (\mathrm{Sh}(c_1), \ldots, \mathrm{Sh}(c_k))$. The *shadow* of an m-painted n-tree $\mathbb{T} := (T, C, \mu)$ is the m-lighted n-shade $\mathrm{Sh}(\mathbb{T}) := (\mathrm{Sh}(S), \mathrm{Sh}(C), \mu)$.

Definition 35. The *shadow congruence* is the equivalence class on m-painted n-trees whose equivalence classes are the fibers of the shadow map. In other words, two m-painted n-trees are shadow congruent if they have the same shadow.

Given two meet semilattices $(M, \wedge)$ and $(M', \wedge')$, a map $f : M \to M'$ is a *meet semilattice morphism* if $f(x \wedge y) = f(x) \wedge' f(y)$ for all $x, y \in M$. The fibers of f are the classes of a *meet semilattice congruence* $\equiv_f$ on M, and the image of f is then called the *meet semilattice quotient* of M by $\equiv_f$. In other words, an equivalence relation $\equiv$ on M is a meet semilattice congruence when $x_1 \equiv x_2$ and $y_1 \equiv y_2$ implies $x_1 \wedge y_1 \equiv x_2 \wedge y_2$, and the quotient $M/\equiv$ is the meet semilattice on the $\equiv$-equivalence classes, where for two $\equiv$-equivalence classes X and Y,

- the order relation is given by $X \leq Y$ if there exist representatives $x \in X$ and $y \in Y$ such that $x \leq y$,
- the meet $X \wedge Y$ is the $\equiv$-equivalence class of $x \wedge y$ for any representatives $x \in X$ and $y \in Y$.

The following classical criterion will be fundamental.

Proposition 36. *An equivalence relation $\equiv$ on a meet semilattice $(M, \wedge)$ is a meet semilattice congruence if and only if*

- *each $\equiv$-equivalence class admits a unique minimal element,*
- *the map $\pi_\downarrow : M \to M$ sending an element of M to the minimal element of its $\equiv$-equivalence class is order preserving.*

We will now apply this characterization to the shadow congruence on the binary m-painted n-tree rotation lattice. This will prove along the way that the binary m-painted n-tree rotation poset is a meet semilattice quotient, hence a meetsemilattice, hence a lattice as it is bounded. This completes the proof of Proposition 27.

Proposition 37. *The shadow map is a surjective meet semilattice morphism from the binary m-painted n-tree rotation lattice to the unary m-lighted n-shade rotation lattice.*

Proof. The shadow fiber of a unary m-lighted n-shade $\mathbb{S} := (S, C, \mu)$ clearly has a unique minimal element (obtained by replacing each element x of S by a left comb on x leaves, cut at the level of its leaves by all lines of C below x).

Consider now two m-painted n-trees $\mathbb{T} := (T, C, \mu)$ and $\mathbb{T}' := (T', C', \mu')$ connected by a right rotation. If this rotation does not affect the right branch of $\mathbb{T}$, then $\mathbb{T}$ and $\mathbb{T}'$ are shadow congruent, so that $\pi_\downarrow(\mathbb{T}) = \pi_\downarrow(\mathbb{T}')$. Assume now that this rotation affects the right branch. There are three possible such flips:

(i) Assume first that we rotate an edge $i \to j$ in $\mathbb{T}$ (with j on the right branch of $\mathbb{T}$) to an edge $i \leftarrow j$ in $\mathbb{T}'$ (with both i and j on the right branch of $\mathbb{T}'$). Then $\pi_\downarrow(\mathbb{T})$ and $\pi_\downarrow(\mathbb{T}')$ coincide except that $\pi_\downarrow(\mathbb{T})$ has a left comb at j (cut at the level of its leaves by all lines of C below j) while $\pi_\downarrow(\mathbb{T}')$ has a left comb at i and a left comb at j (both cut at the level of their leaves by all lines of C below j). As the left comb is the rotation minimal binary tree, we can perform a sequence of right rotations in $\pi_\downarrow(\mathbb{T})$ to obtain $\pi_\downarrow(\mathbb{T}')$. Note here that it is crucial that the cuts appear in the left combs of $\pi_\downarrow(\mathbb{T})$ and $\pi_\downarrow(\mathbb{T}')$ at the level of their leaves so that these binary tree rotations are indeed painted tree rotations.

(ii) Assume now that we sweep a binary node i (on the right branch) by a cut c to pass from $\mathbb{T}$ to $\mathbb{T}'$. Then $\pi_\downarrow(\mathbb{T})$ and $\pi_\downarrow(\mathbb{T}')$ coincide except that the left comb at vertex i of $\pi_\downarrow(\mathbb{T})$ is completely above c while the left comb at vertex i of $\pi_\downarrow(\mathbb{T}')$ is completely below c. Hence, we can successively sweep all nodes of the left comb at vertex i of $\pi_\downarrow(\mathbb{T})$ by the cut c to obtain $\pi_\downarrow(\mathbb{T}')$.

(iii) Assume finally that we exchange the labels of two consecutive cuts with no node in between them to pass from $\mathbb{T}$ to $\mathbb{T}'$. Then we can exchange the labels of the same cuts to pass from $\pi_\downarrow(\mathbb{T})$ to $\pi_\downarrow(\mathbb{T}')$, since they are still consecutive and still have no node between them.

In all cases, we obtain that $\pi_\downarrow(\mathbb{T}) < \pi_\downarrow(\mathbb{T}')$. We conclude that $\pi_\downarrow$ is order preserving, so that the shadow map is a meet semilattice morphism by Proposition 36. $\qquad\square$

Example 38. When $m = 0$, we obtain an unusual meet semilattice morphism from the Tamari lattice to the boolean lattice (distinct from the usual lattice morphism given by the canopy map). When $m = 1$, we obtain a meet semilattice morphism from the multiplihedron lattice to the Hochschild lattice, reminiscent of [Pol20].

Remark 39. Note that the shadow map is not a join semilattice morphism. For instance,

$$\mathrm{Sh}\left(1\,\bigtriangleup\,1 \ \vee\ {}_1\bigwedge{}_1 \right) = \mathrm{Sh}\left({}^{1}\!\!\overline{}\!\!{}^{1}\bigwedge \right) = 1\,\Big|\,{}^{1}_{1}\,,$$

while

$$\mathrm{Sh}\left(1\,\bigwedge\,1 \right) \vee \mathrm{Sh}\left({}_1\bigwedge{}_1 \right) = 2\Big|_1 \vee {}^{1}_{1}\Big|_1 = {}^{1}_{1}\Big|_1\,.$$

Note that there is already a counter-example with $(m, n) = (0, 3)$, see Figure 7 (left).

If we tried to apply the (dual) characterization of Proposition 36, we would observe that, even if the fiber of a unary m-lighted n-shade $\mathbb{S} := (S, C, \mu)$ has a unique maximal element (obtained by replacing each element x of S by a right comb on x leaves, cut at the level of its root by all lines of C below x), the projection map $\pi^{\uparrow}$ is not order preserving.

Remark 40. Note that we could also consider the left shadow map, given by the arity sequence on the left branch of the m-painted n-tree. It defines a join semilattice morphism, which is not a meet semilattice morphism. It would also be interesting to consider the map that records the arity sequence along the path from the root to the ith leaf. And of course all intersections of the equivalence relations arising from these arity sequence maps.

Remark 41. Note that it is crucial here that our orientation of the skeleton of the (m, n)-multiplihedron gives advantage to the permutation part over the binary tree part (in other words, that we consider the shuffle of the m-permutahedron with n-associahedron). Indeed, as observed in the proof of Proposition 37, we need that the cuts appear at the level of the leaves of the left combs in $\pi_{\downarrow}(\mathbb{T})$. Had we considered instead the shuffle of the n-associahedron with the m-permutahedron (or equivalently, the shuffle of the m-permutahedron with the anti-n-associahedron), the (left or right) shadow map would be neither a join nor a meet semilattice morphism.

Remark 42. When $m \leq 1$, the shadow map is a surjective meet semilattice morphism from the m-painted n-tree refinement meet semilattice to the m-lighted n-shade refinement meet semilattice. Indeed, the minimal element $\pi_{\downarrow}(\mathbb{T})$ in the shadow class of an m-painted n-tree $\mathbb{T}$ is obtained by contracting all edges between two nodes that are not on the right branch of $\mathbb{T}$. It fails when $m \geq 2$ as edges between two consecutive cuts cannot be contracted.

1.4. **Singletons.** We now study the fibers of the shadow map which consist in a single m-painted n-tree. They are analoguous to the classical singleton permutations used to construct associahedra, see Remark 62.

Definition 43. An (m, n)-*singleton* is a binary m-painted n-tree which is alone in its shadow congruence class.

Proposition 44. *The following conditions are equivalent for a binary m-painted n-tree $\mathbb{T}$:*

  (i) *$\mathbb{T}$ is an (m, n)-singleton,*
 (ii) *each binary node of $\mathbb{T}$ lies on the right branch, or its parent lies on the right branch if it is below the last cut,*
(iii) *each tuple of the shadow $\mathrm{Sh}(\mathbb{T})$ is reduced to a single 1, or either to a single 1 or a single 2 if it is below the last cut.*

Proof. Assume that $\mathbb{T}$ has a binary node i which is not on the right branch, and let j be the parent of i. If j is a unary node contained in a cut c, then sweeping i with c preserves the shadow of $\mathbb{T}$. If j is a binary node not on the right branch, then rotating the edge $i \to j$ preserves the shadow of $\mathbb{T}$. If j is on the right branch but above a cut, sweeping a node in the left branch of j with c

preserves the shadow of $\mathbb{T}$. Finally, if j is on the right branch and below all cuts, then the only possible rotation in the left branch of j modifies the shadow of $\mathbb{T}$. This proves that (i) $\iff$ (ii). Finally, (ii) clearly translates to (iii) via the shadow map. $\qquad\square$

Corollary 45. *The number of singletons of the (m, n)-shadow map is*

$$m! \sum_{k=0}^{n} \binom{m + k - 1}{k} \mathsf{Fib}_{n-k+1},$$

where Fib_k denote the kth Fibonacci number (defined by $\mathsf{Fib}_0 = \mathsf{Fib}_1 = 1$ and $\mathsf{Fib}_{k+2} = \mathsf{Fib}_{k+1} + \mathsf{Fib}_k$ for $k \geq 0$, see `A000045`*). See Table 7 in Appendix A.3 for the first few numbers.*

Proof. To count the number of singletons, we can simply count the number of shadows of singletons. From their description in Proposition 44 (iii), we obtain that the number of such shades with k entries above the last cut is given by $m!\binom{m+k-1}{k}\mathsf{Fib}_{n-k+1}$. Namely, choose the order of the cuts (hence $m!$ choices), insert k tuples reduced to a single 1 before the last cut (hence $\binom{m+k-1}{k}$ choices), and finish with a sequence of tuples reduced to a single 1 or a single 2, whose total sum is $n - k$ (hence Fib_{n-k+1} choices). $\qquad\square$

Example 46. When $m = 0$, the number of singletons is the Fibonacci Fib_n (`A000045`). When $m = 1$, the number of singletons is $\mathsf{Fib}_{n+2} - 1$ (`A000071`).

2. Multiplihedra and Hochschild polytopes

In this section, we construct polyhedral fans and polytopes whose face lattices are isomorphic to the refinement posets on m-painted n-trees and m-lighted n-shades respectively. We start with a brief recollection on polyhedral geometry (Section 2.1). We then present the vertex and facet of the (m, n)-multiplihedron (Section 2.2) and of the (m, n)-Hochschild polytope (Section 2.3). We conclude by gathering all necessary proofs on Hochschild polytopes (Section 2.4).

2.1. **Recollection on polyhedral geometry.** We start with a brief reminder on fans and polytopes, with a particular attention to deformed permutahedra. We invite the reader familiar with these notions to jump directly to Section 2.2.

2.1.1. *Fans and polytopes.* A (polyhedral) *cone* is the positive span $\mathbb{R}_{\geq 0}\boldsymbol{R}$ of a finite set $\boldsymbol{R}$ of vectors of $\mathbb{R}^d$ or equivalently, the intersection of finitely many closed linear half-spaces of $\mathbb{R}^d$. The *faces* of a cone are its intersections with its supporting hyperplanes. The *rays* (resp. *facets*) are the faces of dimension 1 (resp. codimension 1). A cone is *simplicial* if its rays are linearly independent. A (polyhedral) *fan* $\mathcal{F}$ is a set of cones such that any face of a cone of $\mathcal{F}$ belongs to $\mathcal{F}$, and any two cones of $\mathcal{F}$ intersect along a face of both. A fan is *essential* if the intersection of its cones is the origin, *complete* if the union of its cones covers $\mathbb{R}^d$, and *simplicial* if all its cones are simplicial.

A *polytope* is the convex hull of finitely many points of $\mathbb{R}^d$ or equivalently, a bounded intersection of finitely many closed affine half-spaces of $\mathbb{R}^d$. The *faces* of a polytope are its intersections with its supporting hyperplanes. The *vertices* (resp. *edges*, resp. *facets*) are the faces of dimension 0 (resp. dimension 1, resp. codimension 1).

The *normal cone* of a face $\mathbb{F}$ of a polytope $\mathbb{P}$ is the cone generated by the normal vectors to the supporting hyperplanes of $\mathbb{P}$ containing $\mathbb{F}$. Said differently, it is the cone of vectors $\boldsymbol{c}$ of $\mathbb{R}^d$ such that the linear form $\boldsymbol{x} \mapsto \langle\,\boldsymbol{c}\mid\boldsymbol{x}\,\rangle$ on $\mathbb{P}$ is maximized by all points of the face $\mathbb{F}$. The *normal fan* of $\mathbb{P}$ is the set of normal cones of all its faces.

The *Minkowski sum* of two polytopes $\mathbb{P}, \mathbb{Q} \subseteq \mathbb{R}^n$ is the polytope $\mathbb{P}+\mathbb{Q} := \{p + q \mid p \in \mathbb{P}, q \in \mathbb{Q}\}$. The normal fan of $\mathbb{P} + \mathbb{Q}$ is the common refinement of the normal fans of $\mathbb{P}$ and $\mathbb{Q}$. We write $\mathbb{P} = \mathbb{Q} - \mathbb{R}$ when $\mathbb{P} + \mathbb{R} = \mathbb{Q}$.

A *deformation* of a polytope $\mathbb{P}$ is a polytope $\mathbb{Q}$ satisfying the following equivalent conditions:

- the normal fan of $\mathbb{Q}$ coarsens the normal fan of $\mathbb{P}$,
- $\mathbb{Q}$ is a *weak Minkowski summand* of $\mathbb{P}$, *i.e.* there exists a polytope $\mathbb{R}$ and a positive real number λ such that $\lambda\mathbb{P} = \mathbb{Q} + \mathbb{R}$
- $\mathbb{Q}$ can be obtained from $\mathbb{P}$ by gliding its facets in the direction of its normal vectors without passing a vertex.

2.1.2. The braid fan, the permutahedron, and its deformations. We denote by $(e_i)_{i\in[d]}$ the canonical basis of $\mathbb{R}^d$ and we define $\mathbf{1}_X := \sum_{i\in X} e_i$ for $X \subseteq [d]$, and $\mathbf{1} := \mathbf{1}_{[d]}$. All our polytopal constructions will lie in the affine subspace $\mathbb{H}_d := \{x \in \mathbb{R}^d \mid \langle \mathbf{1} \mid x \rangle = \sum_{i\in[d]} x_i = \binom{d+1}{2}\}$, and their normal fans will lie in the vector subspace $\mathbf{1}^\perp := \{x \in \mathbb{R}^d \mid \langle \mathbf{1} \mid x \rangle = 0\}$.

The *braid arrangement* is the arrangement formed by the hyperplanes $\{x \in \mathbf{1}^\perp \mid x_i = x_j\}$ for all $1 \le i < j \le d$. Its regions (*i.e.* the closures of the connected components of the complement of the union of its hyperplanes) are the maximal cones of the *braid fan* $\mathcal{B}_d$. This fan has a k-dimensional cone for each ordered partition of $[d]$ into $k+1$ parts. In particular, it has a region for each permutation of $[d]$, and a ray for each proper nonempty subset of $[d]$. (Note that we work in the subspace $\mathbf{1}^\perp$ of $\mathbb{R}^d$ so that the braid arrangement is essential and indeed has rays.)

The *permutahedron* $\mathbb{P}\text{erm}(d)$ is the polytope defined equivalently as

- the convex hull of the points $\sum_{i\in[n]} i\, e_{\sigma(i)}$ for all permutations σ of $[d]$, see [Sch11],
- the intersection of the hyperplane $\mathbb{H}_d$ with the halfspaces $\{x \in \mathbb{R}^n \mid \sum_{i\in I} x_i \ge \binom{|I|+1}{2}\}$ for all $\varnothing \ne I \subsetneq [n]$, see [Rad52].

The braid fan $\mathcal{B}_d$ is the normal fan of the permutahedron $\mathbb{P}\text{erm}(d)$. When oriented in the direction $\boldsymbol{\omega} := (n, \ldots, 1) - (1, \ldots, n) = \sum_{i\in[n]}(n+1-2i)\, e_i$, the skeleton of the permutahedron $\mathbb{P}\text{erm}(d)$ is isomorphic to the Hasse diagram of the classical weak order on permutations of $[d]$.

2.1.3. Deformed permutahedra. A *deformed permutahedron* (*a.k.a.* polymatroid [Edm70], or generalized permutahedron [Pos09, PRW08]) is a deformation of the permutahedron. The normal fan of a deformed permutahedron is a collection of preposet cones [PRW08]. The *preposet cone* of a preposet $\preccurlyeq$ on $[d]$ is the cone $\{x \in \mathbb{R}^d \mid x_i \le x_j \text{ if } i \preccurlyeq j\}$. For instance, the cones of the braid fan are precisely the preposet cones of the total preposets (*i.e.* those where $i \preccurlyeq j$ or $j \preccurlyeq i$ for any $i, j \in [d]$).

There are two standard parametrizations of the deformed permutahedra. Namely, for a deformed permutahedron $\mathbb{P}$ in $\mathbb{R}^d$, we define:

- its *Minkowski coefficients* $(\boldsymbol{y}_I(\mathbb{P}))_{\varnothing \ne I \subseteq [d]}$ such that $\mathbb{P}$ is the Minkowski sum and difference $\sum_{\varnothing \ne I \subseteq [d]} \boldsymbol{y}_I(\mathbb{P})\, \triangle_I$, where $\triangle_I := \text{conv}\{e_i \mid i \in I\}$ is the face of the standard simplex $\triangle_{[d]} := \text{conv}\{e_i \mid i \in [d]\}$ corresponding to I,
- its *tight right hand sides* $(\boldsymbol{z}_J(\mathbb{P}))_{\varnothing \ne J \subseteq [d]}$ such that $\boldsymbol{z}_J(\mathbb{P}) := \min\{\langle \mathbf{1}_J \mid p \rangle \mid p \in P\}$.

As proved in [Pos09, ABD10], these two parametrizations are related by boolean Möbius inversion:

$$\boldsymbol{z}_J(\mathbb{P}) = \sum_{I\subseteq J} \boldsymbol{y}_I(\mathbb{P}) \qquad \text{and} \qquad \boldsymbol{y}_I(\mathbb{P}) = \sum_{J\subseteq I} (-1)^{|I\smallsetminus J|}\, \boldsymbol{z}_J(\mathbb{P}).$$

For instance, for the classical permutahedron $\mathbb{P}\text{erm}(d)$,

- its Minkowski coefficients are $\boldsymbol{y}_I(\mathbb{P}\text{erm}(d)) = 1$ if $|I| \le 2$ and 0 otherwise,
- its tight right hand sides are $\boldsymbol{z}_J(\mathbb{P}\text{erm}(d)) = \binom{|J|+1}{2}$.

As another illustration, recall that the *n-associahedron* $\mathbb{A}\text{sso}(d)$ is the deformed permutahedron defined equivalently as

- the convex hull of the points $\sum_{i\in[n]} \ell(T,i)\, r(T,i)\, e_i$ for all binary trees T with n internal nodes, where $\ell(T,i)$ and $r(T,i)$ respectively denote the numbers of leaves in the left and right subtrees of the ith node of T in infix labeling, see [Lod04],
- the intersection of the hyperplane $\mathbb{H}_d$ with the halfspaces $\{x \in \mathbb{R}^n \mid \sum_{i\le\ell\le j} x_\ell \ge \binom{j-i+2}{2}\}$ for all $1 \le i \le j \le n$, see [SS93].

Moreover,

- its Minkowski coefficients are $\boldsymbol{y}_I(\mathbb{A}\text{sso}(d)) = 1$ if I is an interval of $[n]$ and 0 otherwise, see [Pos09],
- its tight right hand sides are $\boldsymbol{z}_J(\mathbb{A}\text{sso}(d)) = \binom{|J_1|+1}{2} + \cdots + \binom{|J_k|+1}{2}$ where $J = J_1 \cup \cdots \cup J_k$ is the decomposition of J into maximal intervals of $[n]$, see [Lan13].

2.2. **Multiplihedra.** We now consider the (m, n)-multiplihedron which realize the m-painted n-tree refinement semilattice. These polytopes are illustrated in Figures 1, 17 and 18. Although they were previously constructed when $m = 1$ in [Sta63, SU04, For08, FLS10, MW10, AD13], we use here the construction of [CP22, Sect. 3]. This construction is just an example of the shuffle product on deformed permutahedra, introduced in [CP22, Sect. 2]. However, we do not really need the generality of this operation and define here the (m, n)-multiplihedron using its vertex and facet descriptions.

Definition 47. Consider a binary m-painted n-tree $\mathbb{T} := (T, C, \mu)$. We associate to $\mathbb{T}$ a point $\boldsymbol{a}(\mathbb{T})$ whose pth coordinate is

- if $p \leq m$, the number of binary nodes and cuts weakly below the cut labeled by p,
- if $p \geq m + 1$, the number of cuts below plus the product of the numbers of leaves in the left and right subtrees the node of T labeled by $p - m$ in inorder.

See Figure 13 for some examples.

Definition 48. Consider the hyperplane $\mathbb{H}_{m+n}$ of $\mathbb{R}^{m+n}$ defined by the equality

$$\left\langle \boldsymbol{x} \mid \mathbf{1}_{[m+n]} \right\rangle = \binom{m + n + 1}{2}.$$

Moreover, for each rank $m + n - 2$ m-painted n-tree $\mathbb{T} := (T, C, \mu)$, consider the halfspace $\boldsymbol{H}(\mathbb{T})$ of $\mathbb{R}^{m+n}$ defined by the inequality

$$\left\langle \boldsymbol{x} \mid \mathbf{1}_{A \cup B} \right\rangle \geq \binom{|A| + 1}{2} + \binom{|B_1| + 1}{2} + \cdots + \binom{|B_k| + 1}{2} + |A| \cdot |B|,$$

where

- A denotes the set of elements of $[m]$ which label the cut not containing the root of T (hence, $A = \varnothing$ if C has only one cut, which contains the root of T),
- $B := B_1 \cup \cdots \cup B_k$ where $B_1, \ldots, B_k$ are the inorder labels shifted by m of the non-unary nodes of T distinct from the root of T.

See Figure 14 for some examples.

Proposition 49 ([CP22, Props. 116, 122, 123]). *The m-painted n-tree refinement lattice is anti-isomorphic to the face lattice of the (m, n)-multiplihedron $\mathbb{Mul}(m, n)$, defined equivalently as*

- *the convex hull of the vertices $\boldsymbol{a}(\mathbb{T})$ for all binary m-painted n-trees $\mathbb{T}$,*
- *the intersection of the hyperplane $\mathbb{H}_{m+n}$ with the halfspaces $\boldsymbol{H}(\mathbb{T})$ for all rank $m + n - 2$ m-painted n-trees $\mathbb{T}$.*

Proposition 50 ([CP22, Prop. 118]). *The normal fan of the (m, n)-multiplihedron $\mathbb{Mul}(m, n)$ is the fan whose cones are the preposet cones of the preposets $\preccurlyeq_{\mathbb{T}}$ of all m-painted n-trees $\mathbb{T}$.*

Proposition 51 ([CP22, Prop. 119]). *When oriented in the direction $\boldsymbol{\omega} := (n, \ldots, 1) - (1, \ldots, n)$, the skeleton of the (m, n)-multiplihedron $\mathbb{Mul}(m, n)$ is isomorphic to the right rotation digraph on binary m-painted n-trees.*

Remark 52. As observed in [CP22, Prop. 124], it is straightforward to obtain the $\boldsymbol{y}$ and $\boldsymbol{z}$ parametrizations of the (m, n)-multiplihedron $\mathbb{Mul}(m, n)$. Namely, for $I \subseteq [m + n]$, we have

$$\boldsymbol{y}_I\big(\mathbb{Mul}(m, n)\big) = \begin{cases} 1 & \text{if } |I| \leq 2 \text{ and } |I \cap [n]^{+m}| \leq 1, \text{ or } I \text{ is a subinterval of } [n]^{+m} \\ 0 & \text{otherwise} \end{cases}$$

and

$$\boldsymbol{z}_J\big(\mathbb{Mul}(m, n)\big) = \binom{|A| + 1}{2} + \binom{|B_1| + 1}{2} + \cdots + \binom{|B_k| + 1}{2} + |A| \cdot |B|,$$

where $A := J \cap [m]$ and $B := B_1 \cup \cdots \cup B_k$ is the coarsest interval decomposition of $J \smallsetminus [m]$.

Example 53. When $m = 0$, the $(0, n)$-multiplihedron is Loday's associahedron [Lod04]. When $m = 1$, the $(1, n)$-multiplihedron is the classical multiplihedron alternatively constructed in [For08, AD13].
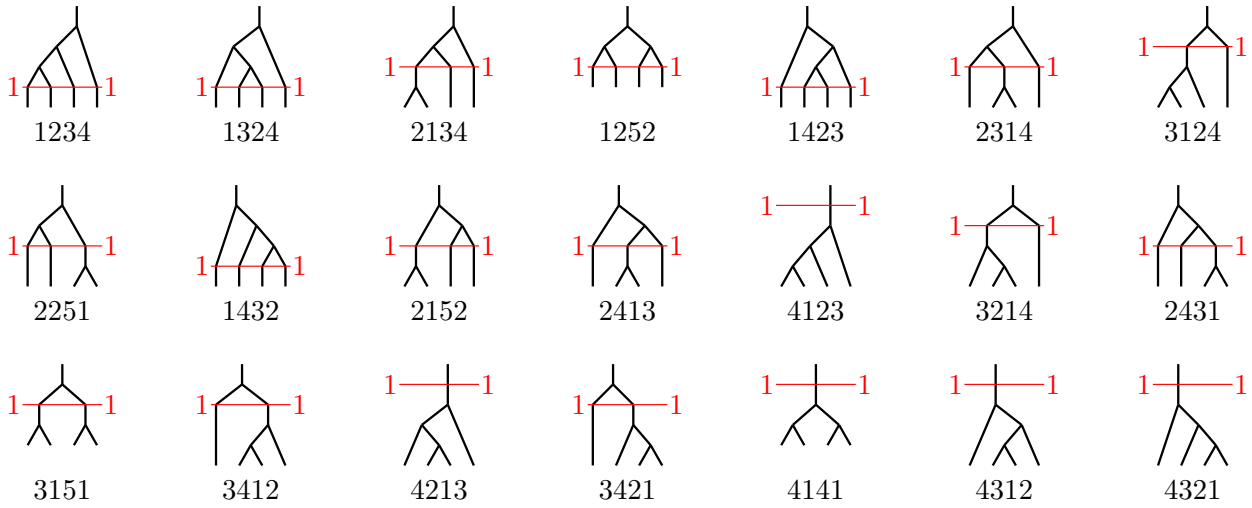
FIGURE 13. Vertices of $\mathbb{Mul}(1,3)$.

$x_1 \geq 1$ $x_1 + x_2 \geq 3$ $x_1 + x_3 \geq 3$ $x_1 + x_4 \geq 3$ $x_1 + x_2 \atop +x_3 \geq 6$ $x_1 + x_2 \atop +x_4 \geq 5$ $x_1 + x_3 \atop +x_4 \geq 6$

$x_2 \geq 1$ $x_3 \geq 1$ $x_4 \geq 1$ $x_2 + x_3 \geq 3$ $x_3 + x_4 \geq 3$ $x_2 + x_3 \atop +x_4 \geq 6$
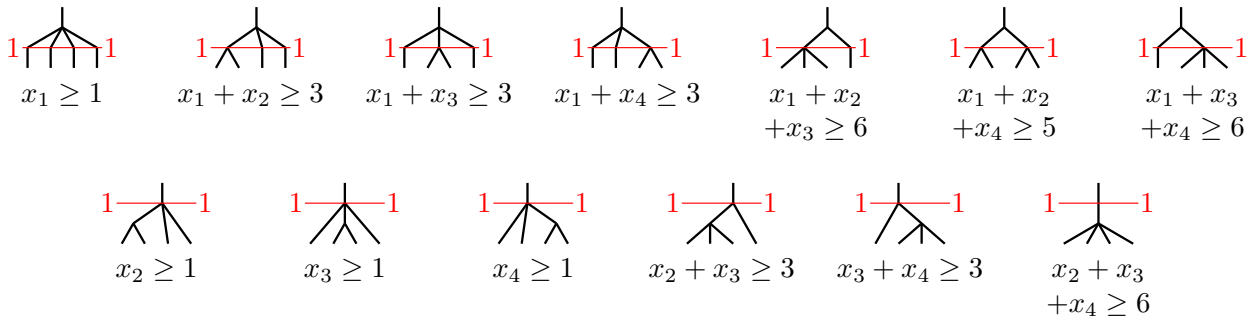
FIGURE 14. Facet defining inequalities of $\mathbb{Mul}(1,3)$.

1117   1162   1414   2161   1432   4114   2431   3412   3421   4141   4312   4321
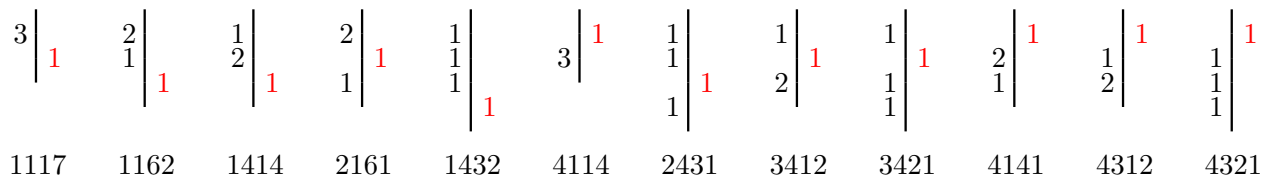
FIGURE 15. Vertices of $\mathbb{Hoch}(1,3)$.

$x_1 \geq 1$ $x_1 + x_4 \geq 3$ $x_1 + x_3 \atop +x_4 \geq 6$ $x_2 \geq 1$ $x_3 \geq 1$ $x_4 \geq 1$ $x_3 + x_4 \geq 1$ $x_2 + x_3 \atop +x_4 \geq 6$

FIGURE 16. Facet defining inequalities of $\mathbb{Hoch}(1,3)$.

2.3. **Hochschild polytopes.** We now construct the (m, n)-Hochschild polytope which realize the m-lighted n-shade refinement semilattice. These polytpes are illustrated in Figures 1, 17 and 18. Recall that we denote by $ps(x)$ the preceeding sum of an entry x in an m-lighted n-shade (see Definition 19).

Definition 54. Consider a unary m-lighted n-shade $\mathbb{S} := (S, C, \mu)$ and denote by $s_1, s_2, \ldots, s_k$ the values of the singleton tuples of S. We associate to $\mathbb{S}$ a point $\boldsymbol{a}(\mathbb{S})$ whose pth coordinate is

- if $p \leq m$, then the number of cuts plus the sum of the entries s_i which are weakly below the cut labeled p,
- if there is $j \in [k]$ such that $p = ps(s_j)$, then $1 + s_j(m + n - p + c_p) + \binom{s_j}{2}$ where c_p is the number of cuts below s_j.
- 1 otherwise.

See Figure 15 for some examples.

Definition 55. We still denote by $\mathbb{H}_{m+n}$ the hyperplane of $\mathbb{R}^{m+n}$ defined by the equality

$$\left\langle\, \boldsymbol{x} \mid \boldsymbol{1}_{[m+n]} \,\right\rangle = \binom{m+n+1}{2}.$$

Moreover, for each rank $m + n - 2$ m-lighted n-shade $\mathbb{S} := (S, C, \mu)$, consider the halfspace $\boldsymbol{H}(\mathbb{S})$ of $\mathbb{R}^{m+n}$ defined by the inequality

$$\left\langle\, \boldsymbol{x} \mid \boldsymbol{1}_{A \cup B} \,\right\rangle \geq \binom{|A| + |B| + 1}{2},$$

where

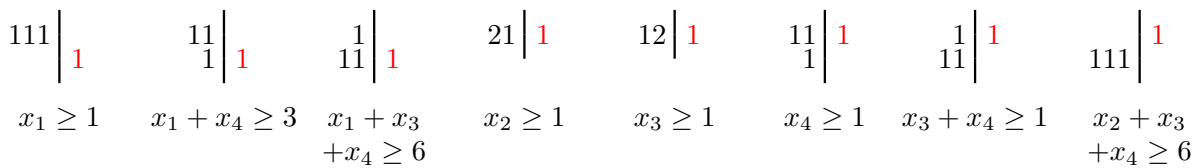- A denotes the set of elements of $[m]$ which label the cut not containing the first tuple of S (hence, $A = \varnothing$ if C has only one cut, which contains the first tuple of S),
- $B = \{m+q\}$ if S is a single tuple with the 2 in position q, and $B = \{m+q+1, \ldots, m+n\}$ if $S = (s_1, s_2)$ is a pair of tuples with $|s_1| = q$.

See Figure 16 for some examples.

Remark 56. The inequalities of Definition 55 form a subset of the inequalities of Definition 48.

We postpone the proofs of the next three statements to Section 2.4.

Proposition 57. *The m-lighted n-shade refinement lattice is anti-isomorphic to the face lattice of the (m, n)-Hochschild polytope $\mathbb{H}\mathrm{och}(m, n)$, defined equivalently as*

(i) *the convex hull of the vertices $\boldsymbol{a}(\mathbb{S})$ for all unary m-lighted n-shades $\mathbb{S}$,*
(ii) *the intersection of the hyperplane $\mathbb{H}_{m+n}$ with the halfspaces $\boldsymbol{H}(\mathbb{S})$ for all rank $m + n - 2$ m-lighted n-shades $\mathbb{S}$.*

Proposition 58. *The normal fan of the (m, n)-Hochschild polytope $\mathbb{H}\mathrm{och}(m, n)$ is the fan whose cones are the preposet cones of the preposets $\preccurlyeq_{\mathbb{S}}$ of all m-lighted n-shades $\mathbb{S}$.*

Proposition 59 ([CP22, Prop. 119]). *When oriented in the direction $\boldsymbol{\omega} := (n, \ldots, 1) - (1, \ldots, n)$, the skeleton of the (m, n)-Hochschild polytope $\mathbb{H}\mathrm{och}(m, n)$ is isomorphic to the right rotation digraph on unary m-lighted n-shades.*

Remark 60. It follows from Remarks 20 and 26 that the (m, n)-Hochschild polytope is simple and the m-lighted n-shade fan is simplicial. This will simplify our proofs in Section 2.4.

Remark 61. As in Remark 52, one can compute the $\boldsymbol{y}$ and $\boldsymbol{z}$ parametrizations of the (m, n)-Hochschild polytope $\mathbb{H}\mathrm{och}(m, n)$. Namely, for $I \subseteq [m + n]$, we have

$$\boldsymbol{y}_I\big(\mathbb{H}\mathrm{och}(m, n)\big) = \begin{cases} 1 & \text{if } |I| = 1, \text{ or } |I| = 2 \text{ and } I \subseteq [m], \\ & \text{or } I = \{i, m+j, m+j+1, \ldots, m+n\} \text{ for some } i \in [m] \text{ and } j \in [n] \\ n - j & \text{if } I = \{m+j, m+j+1, \ldots, m+n\} \text{ for some } j \in [n] \\ 0 & \text{otherwise} \end{cases}$$

FIGURE 17. The multiplihedron $\mathbb{Mul}(m, n)$ (top) and the Hochschild polytope $\mathbb{Hoch}(m, n)$ (bottom) for $(m, n) = (0, 3)$, $(1, 2)$, $(2, 1)$, and $(3, 0)$ (left to right).

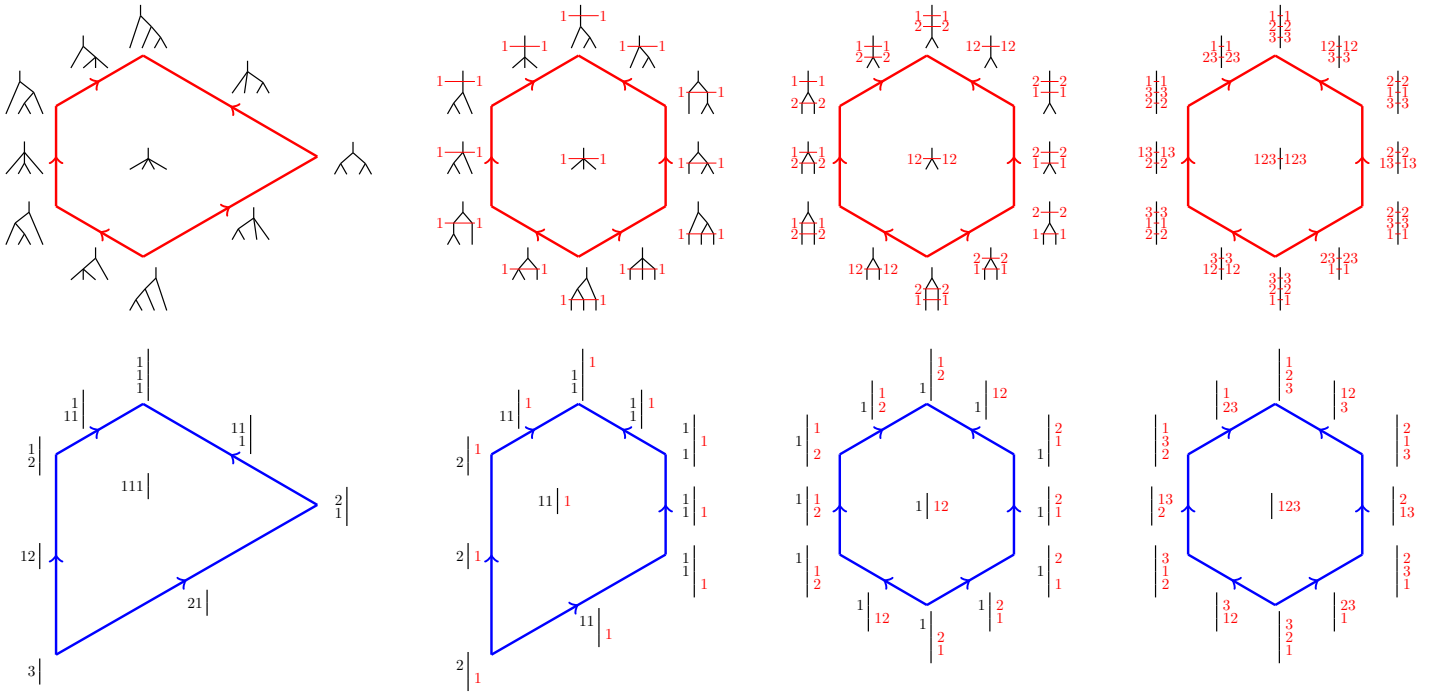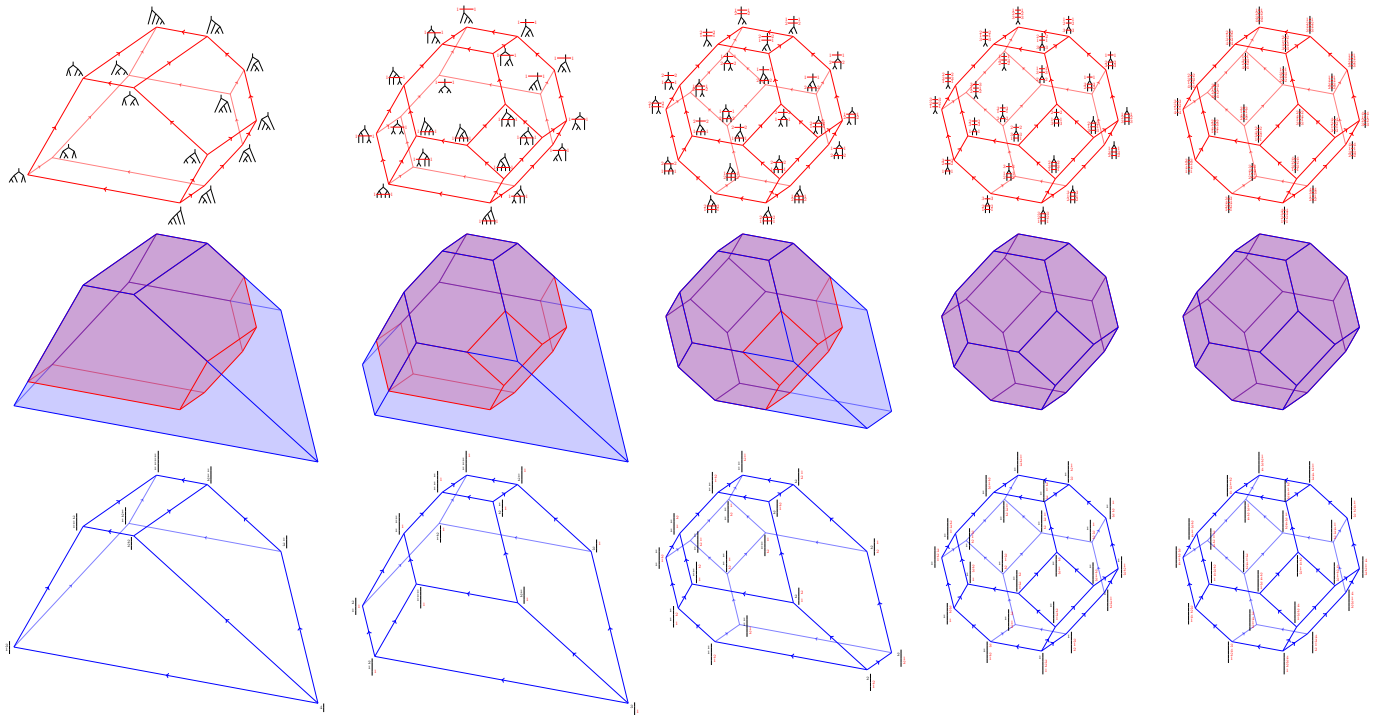FIGURE 18. The multiplihedron $\mathbb{Mul}(m, n)$ (top) and the Hochschild polytope $\mathbb{Hoch}(m, n)$ (bottom) for $(m, n) = (0, 4)$, $(1, 3)$, $(2, 2)$, $(3, 1)$, and $(4, 0)$ (left to right).
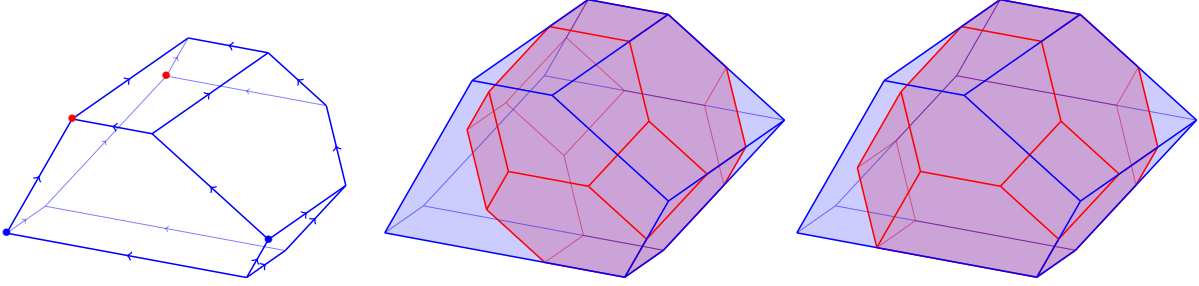
FIGURE 19. The freehedron obtained as Minkowski sum of the faces of the standard simplex corresponding to initial or final intervals (left), and failed attempts to obtain it as a removahedron of the permutahedron (middle) or of the multiplihedron (right).

and

$$\boldsymbol{z}_J\big(\mathbb{Hoch}(m,n)\big) = \binom{|A| + |C| + 1}{2} + |B|,$$

where $A := J \cap [m]$, and $B \cup C := J \smallsetminus [m]$ such that C is the largest interval of $J \smallsetminus [m]$ containing $m+n$.

Remark 62. As mentioned in the introduction, there are deep similarities between the behaviors of

- the permutahedron $\mathbb{Perm}(d)$ and the associahedron $\mathbb{Asso}(d)$,
- the multiplihedron $\mathbb{Mul}(m,n)$ and the Hochschild polytope $\mathbb{Hoch}(m,n)$.

We conclude with a few comments on the behavior of the later for the reader familiar with the behavior of the former:

- As observed in Remark 56, the (m,n)-Hochschild polytope $\mathbb{Hoch}(m,n)$ can be obtained by deleting inequalities in the facet description of the (m,n)-multiplihedron $\mathbb{Mul}(m,n)$.
- The common facet defining inequalities of $\mathbb{Mul}(m,n)$ and $\mathbb{Hoch}(m,n)$ are precisely those that contain a common vertex of $\mathbb{Mul}(m,n)$ and $\mathbb{Hoch}(m,n)$ (the singletons of Section 1.4).
- In contrast, the vertex barycenters of the (m,n)-multiplihedron $\mathbb{Mul}(m,n)$ and of the (m,n)-Hochschild polytope $\mathbb{Hoch}(m,n)$ do not coincide.
- When $m = 0$, the $(0,n)$-Hochschild polytope $\mathbb{Hoch}(0,n)$ is a skew cube distinct from the parallelepiped obtained by considering the canopy congruence on binary trees (which is a lattice congruence, in contrast to the shadow meet semilattice congruence).

Example 63. When $m = 0$, the $(0,n)$-Hochschild polytope is a skew cube. Note that it is distinct from the parallelotope $\sum_{i\in[n-1]}[\boldsymbol{e}_i, \boldsymbol{e}_{i+1}]$. When $m = 1$, the $(1,n)$-Hochschild polytope gives a realization of the Hochschild lattice [Cha20, Com21, Müh22]. Note that the unoriented rotation graph on 1-lighted n-shades was already known to be isomorphic to the unoriented skeleton of a deformed permutahedron called *freehedron* and obtained as a truncation of the standard simplex [San09], or more precisely as the Minkowski sum $\sum_{i\in[n]} \triangle_{\{1,\dots,i\}} + \sum_{i\in[n]} \triangle_{\{i,\dots,n\}}$ of the faces of the standard simplex corresponding to initial and final intervals, see Figure 19. However, orienting the skeleton of the freehedron in direction $\boldsymbol{\omega}$, we obtain a poset different from the Hochschild lattice, and which is not even a lattice. Indeed, in Figure 19 (left) the two blue vertices have no join while the two red vertices have no meet. In fact, the Hasse diagram of the Hochschild lattice cannot be obtained as a Morse orientation given by a linear functional on the freehedron. Finally, observe that the freehedron cannot be obtained by removing inequalities in the facet description of the permutahedron or of the multiplihedron. See Figure 19 (middle and right) where the resulting removahedra have the wrong combinatorics (look at the 4-valent vertex on the right of the polytopes).

2.4. **Proof of Propositions 51, 57 and 58.** Our proof strategy follows that of [HLT11, Sect. 4]. First, we will prove that the collection of cones described in Proposition 58 indeed defines a fan.

Proposition 64. *The preposets cones of the preposets $\preccurlyeq_{\mathbb{S}}$ for all m-lighted n-shades $\mathbb{S}$ define a complete simplicial fan realizing the m-lighted n-shade refinement semilattice.*

Proof. By Remark 20, the Hasse diagram of the preposets $\preccurlyeq_{\mathbb{S}}$ of each m-lighted n-shade $\mathbb{S}$ is a forest, so that the corresponding preposet cone is simplicial. Moreover, contracting any edge in this forest gives rise to the Hasse diagram of the preposet $\preccurlyeq_{\mathbb{S}'}$ of an m-lighted n-shade $\mathbb{S}'$ refined by $\mathbb{S}$, so that this collection of cones is closed by faces. Finally, we have a well-defined shadow map Sh, which sends an m-painted n-tree $\mathbb{T}$ to the refinement maximal m-lighted n-shade $\mathbb{S}$ such that $\preccurlyeq_{\mathbb{T}} \subseteq \preccurlyeq_{\mathbb{S}}$. Since the preposet cones of the preposets $\preccurlyeq_{\mathbb{T}}$ for all m-painted n-trees $\mathbb{T}$ form a complete fan $\mathcal{F}$, we conclude that the preposets cones of the preposets $\preccurlyeq_{\mathbb{S}}$ for all m-lighted n-shades $\mathbb{S}$ also form a complete fan refined by $\mathcal{F}$. $\square$

Next, we apply the following characterization to realize a complete simplicial fan as the normal fan of a convex polytope. A proof of this statement can be found *e.g.* in [HLT11, Theorem 4.1].

Theorem 65 ([HLT11, Thm 4.1])**.** *Consider a complete simplicial fan $\mathcal{F}$ in $\mathbb{R}^d$, and choose*

- *a point $\boldsymbol{a}(C)$ for each maximal cone C of $\mathcal{F}$,*
- *a half-space $\boldsymbol{H}(\rho)$ of $\mathbb{R}^d$ containing the origin for each ray ρ of $\mathcal{F}$,*

such that $\boldsymbol{a}(C)$ belongs to the hyperplane defining $\boldsymbol{H}^{=}(\rho)$ when $\rho \in C$. Then the following assertions are equivalent:

- *the vector $\boldsymbol{a}(C') - \boldsymbol{a}(C)$ points from C to C' for any two adjacent maximal cones C, C' of $\mathcal{F}$,*
- *the polytopes*

$$\mathrm{conv}\,\{\boldsymbol{a}(C) \mid C \text{ maximal cone of } \mathcal{F}\} \qquad and \qquad \bigcap_{\rho \text{ ray of } \mathcal{F}} \boldsymbol{H}(\rho)$$

coincide and their normal fan is $\mathcal{F}$.

In the next two lemmas, we check the conditions of application of Theorem 65.

Lemma 66. *For any m-lighted n-shades $\mathbb{S}$ and $\mathbb{S}'$, of rank 0 and $m+n-2$ respectively, such that $\preccurlyeq_{\mathbb{S}}$ refines $\preccurlyeq_{\mathbb{S}'}$, the point $\boldsymbol{a}(\mathbb{S})$ belongs to the hyperplane defining $\boldsymbol{H}(\mathbb{S}')$.*

Proof. Denote by $s_1, \ldots, s_k$ the values of the singleton tuples of $\mathbb{S}$. We distinguish two cases:

- Assume first that $\mathbb{S}'$ contains a single tuple with the 2 in position q, so that $A = \varnothing$ and $B = \{m+q\}$ in Definition 48. Since $\mathbb{S}$ refines $\mathbb{S}'$, there is no j so that $m+q = ps(s_j)$, so that $\boldsymbol{a}(\mathbb{S})_{m+q} = 1$ in Definition 47. We conclude that

$$\langle\, \boldsymbol{a}(\mathbb{S}) \mid \mathbf{1}_{A \cup B}\,\rangle = \boldsymbol{a}(\mathbb{S})_{m+q} = 1 = \binom{|A| + |B| + 1}{2}.$$

- Assume now that $\mathbb{S}'$ is a pair of tuples (s_1', s_2') with $|s_1'| = q$, so that $A \subseteq [m]$ are the labels of the cut containing s_2', and $B = \{m+q+1, \ldots, m+n\}$ in Definition 48. Since $\mathbb{S}$ refines $\mathbb{S}'$, there is j such that $q = ps(s_j)$. We conclude that

$$\langle\, \boldsymbol{a}(\mathbb{S}) \mid \mathbf{1}_{A \cup B}\,\rangle = \binom{|A| + 1}{2} + |A||B| + \sum_{i=j+1}^{k} \left(s_i - 1 + s_i\big(n - ps(s_i)\big) + \binom{s_i}{2}\right)$$

$$= \binom{|A| + 1}{2} + |A||B| + \binom{|B| + 1}{2} = \binom{|A| + |B| + 1}{2}. \qquad \square$$

We now check that for a rotation sending $\mathbb{S}$ to $\mathbb{S}'$, the direction between the two points $\boldsymbol{a}(\mathbb{S})$ and $\boldsymbol{a}(\mathbb{S}')$ of Definition 47 points from the poset cone $\preccurlyeq_{\mathbb{S}}$ to the poset cone $\preccurlyeq_{\mathbb{S}'}$ of Definition 19.

Lemma 67. *For any unary m-lighted n-shades $\mathbb{S}$ and $\mathbb{S}'$ related by a rotation, the vector $\boldsymbol{a}(\mathbb{S}') - \boldsymbol{a}(\mathbb{S})$ points from the poset cone $\preccurlyeq_{\mathbb{S}}$ to the poset cone $\preccurlyeq_{\mathbb{S}'}$.*

Proof. We distinguish three cases according to Remark 25. Namely, if we obtain $\mathbb{S}'$ from $\mathbb{S}$ by:

(i) replacing a singleton (r) by two singletons $(s), (t)$ with $r = s + t$, then

$$\boldsymbol{a}(\mathbb{S}') - \boldsymbol{a}(\mathbb{S}) = \big(s(m + n - p + t + c_p) + \tbinom{s}{2}\big)(\boldsymbol{e}_{p-t} - \boldsymbol{e}_p),$$

and we have $p - t \prec_{\mathbb{S}} p$ while $p \prec_{\mathbb{S}'} p - t$, where $p := ps(r)$ is the preceeding sum of r in $\mathbb{S}$.

(ii) exchanging a singleton (s) with a cut c (with (s) above c in $\mathbb{S}$), then $\boldsymbol{a}(\mathbb{S}') - \boldsymbol{a}(\mathbb{S}) = \boldsymbol{e}_c - \boldsymbol{e}_p$ and we have $c \prec_{\mathbb{S}} p$ while $p \prec_{\mathbb{S}'} c$, where $p := ps(s)$.

(iii) exchanging the labels of two consecutive cuts c, c' with no singleton in between them (with c above c' in $\mathbb{S}$), then $\boldsymbol{a}(\mathbb{S}') - \boldsymbol{a}(\mathbb{S}) = \boldsymbol{e}_{c'} - \boldsymbol{e}_c$ and we have $c' \prec_{\mathbb{S}} c$ while $c \prec_{\mathbb{S}'} c'$.

In all cases, the vector $\boldsymbol{a}(\mathbb{S}') - \boldsymbol{a}(\mathbb{S})$ points from the poset cone $\preccurlyeq_{\mathbb{S}}$ to the poset cone $\preccurlyeq_{\mathbb{S}'}$. $\square$

Proof of Propositions 51, 57 and 58. We have seen in Proposition 64 that the preposet cones of the preposets $\preccurlyeq_{\mathbb{S}}$ for all m-lighted n-shades $\mathbb{S}$ define a complete simplicial fan. By Theorem 65, whose conditions of application are checked in Lemmas 66 and 67, we thus obtain Propositions 57 and 58. Finally, Proposition 51 is a direct consequence of Lemma 67, since $\langle \boldsymbol{a}(\mathbb{S}') - \boldsymbol{a}(\mathbb{S}) \mid \boldsymbol{\omega} \rangle > 0$ for $\mathbb{S}$ and $\mathbb{S}'$ related by a right rotation. $\square$

3. Cubic realizations

In this section we give an alternative description of the m-painted n-tree and m-lighted n-shade rotation lattices, generalizing the triword description of the Hochschild lattice [Cha20, Com21, Müh22]. We also construct the cubic subdivisions realizing the face poset of the (m, n)-multiplihedron and of the (m, n)-Hochschild polytope, generalizing the original construction of [San09, RS18]. We first fix our conventions and give examples of cubic realizations (Section 3.1), then recall the cubic (m, n)-multiplihedron (Section 3.2) and finally construct the cubic (m, n)-Hochschild polytope (Section 3.3).

3.1. **Cubic realizations of posets.** We first propose formal definitions of two types of cubic realizations of posets. The first is the cubic analogue of the face lattice of a polytope while the second is the cubic analogue of the oriented skeleton of a polytope. These definitions are illustrated in Examples 70 and 71 with the permutahedron and the associahedron.

Definition 68. We call *cube* any axis parallel parallelepiped in $\mathbb{R}^d$. If $\boldsymbol{x}, \boldsymbol{y} \in \mathbb{R}^d$ are such that $x_i \leq y_i$ for all $i \in [d]$, we denote by $\mathrm{Cube}(\boldsymbol{x}, \boldsymbol{y})$ the cube $\prod_{i \in [d]} [x_i, y_i]$. A *subcube* of C is a cube included in C whose vertices all lie on the boundary of C. A *cubic subdivision* of C is a collection $\mathcal{D}$ of subcubes of C such that

- The boundary of C is the union of all the subcubes of $\mathcal{D}$,
- for any subcubes $C', C'' \in \mathcal{D}$, the intersection $C' \cap C''$ is either empty or a subcube of $\mathcal{D}$, with $\dim(C' \cap C'') < \min(\dim(C), \min(C'))$.

The *subcube poset* of the cubic subdivision $\mathcal{D}$ is the poset on $\mathcal{D} \cup \{C\}$ ordered by inclusion. A cubic subdivision *realizes* a poset P if its subcube poset is isomorphic to P.

Definition 69. A *cubic realization* of a poset P is a map $\gamma : P \to \mathbb{R}^d$ such that

- for any cover relation $p \lessdot q$ in P, the difference $\gamma(p) - \gamma(q)$ is a positive multiple of some basis vector $\boldsymbol{e}_i$,
- $\gamma(P)$ lies on the boundary of $\mathrm{Cube}\big(\gamma(\min(P)), \gamma(\max(P))\big)$.

Note that our conventions are slightly unusual: we require that the cubic coordinates are decreasing along the poset, so that the maximum of the poset P has minimal cubic coordinates. Our choice is driven by the fact that we want our cubic coordinates for 1-lighted n-shades to coincide with the triwords of [San09, RS18, Cha20, Com21, Müh22]. We next illustrate these two notions of cubic realizations with the Lehmer code of a permutation and the bracket vector of a binary tree (or we should say adaptations of them, in order to stick with our conventions).
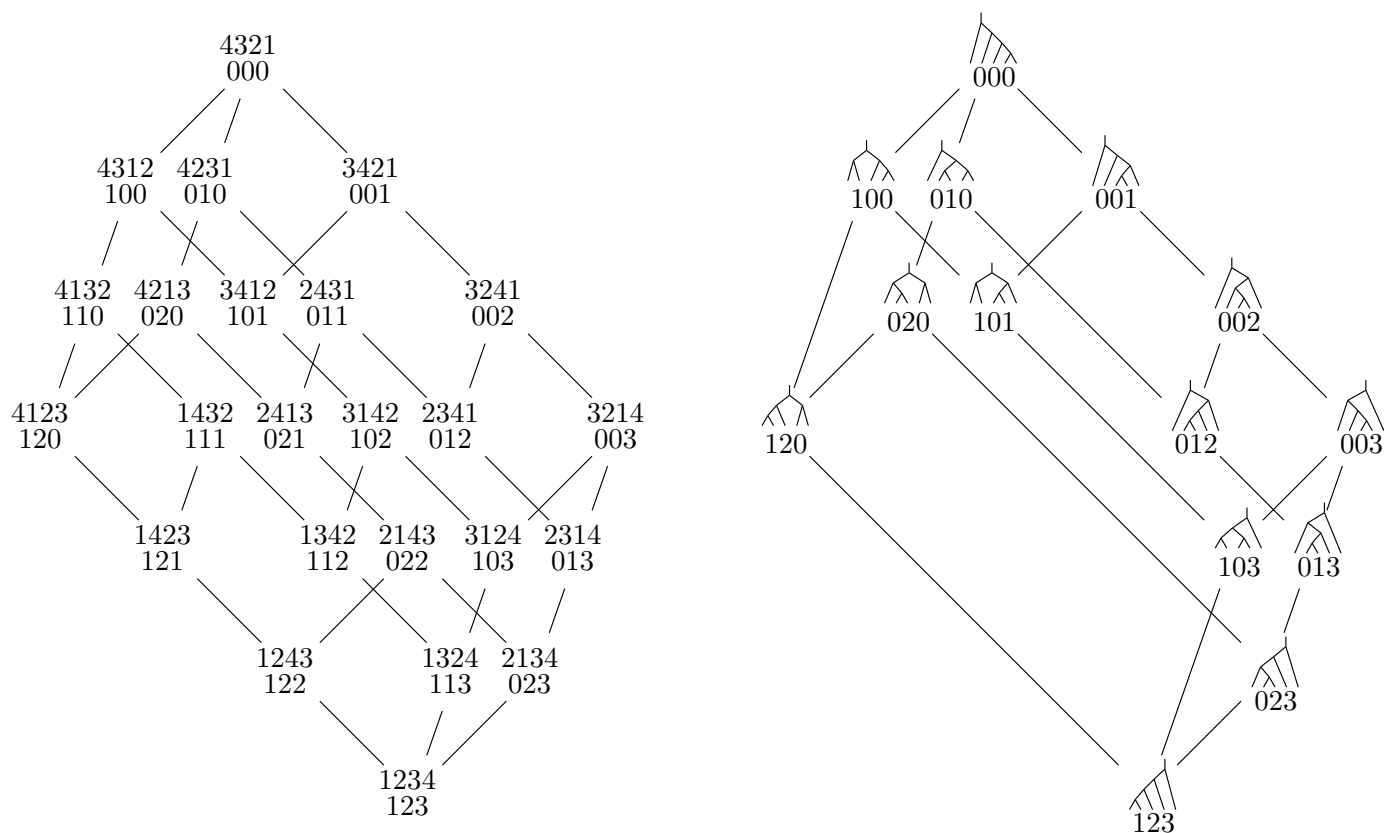
FIGURE 20. Cubic realizations of the weak order via the Lehmer codes of permutations (left) and of the Tamari lattice via the bracket vectors of binary trees (right).

Example 70. The *Lehmer code* [Leh60] of a permutation σ of $[m]$ is the vector $\boldsymbol{L}(\sigma) := \big(L_j(\sigma)\big)_{j \in [m]}$ where $L_j(\sigma) = \#\big\{i < j \mid \sigma^{-1}(i) < \sigma^{-1}(j)\big\}$. Note that $L_j(\sigma) \in \{0, \ldots, j-1\}$, so that it is standard to forget the first coordinate (which is always 0). These Lehmer codes define

- a cubic realization of the weak order on the permutations of $[m]$,
- a cubic subdivision realizing the face lattice of the permutahedron $\mathbb{P}\mathrm{erm}(d)$ by the set of cubes $\mathrm{Cube}\big(\boldsymbol{L}(\sigma), \boldsymbol{L}(\tau)\big)$ for $\sigma \leq \tau$ defining a face of $\mathbb{P}\mathrm{erm}(d)$.

See Figure 20 (left) for illustration.

Example 71. The *bracket vector* [HT72] of a binary tree T with n internal nodes is the vector $\boldsymbol{B}(T) := \big(B_j(T)\big)_{j \in [n]}$ where $B_j(T)$ is the number of descendants of j which are smaller than j (for the usual inorder labeling of T). Equivalently, $B_j(T)$ is the number of leaves minus 1 in the left subtree of i. Note that $B_j(\sigma) \in \{0, \ldots, j-1\}$, so that it is standard to forget the first coordinate (which is always 0). The bracket vectors define

- a cubic realization of the Tamari lattice on the binary trees with n nodes,
- a cubic subdivision realizing the face lattice of the associahedron $\mathbb{A}\mathrm{sso}(d)$ by the set of cubes $\mathrm{Cube}\big(\boldsymbol{B}(S), \boldsymbol{B}(T)\big)$ for $S \leq T$ defining a face of $\mathbb{A}\mathrm{sso}(d)$.

See Figure 20 (right) for illustration.
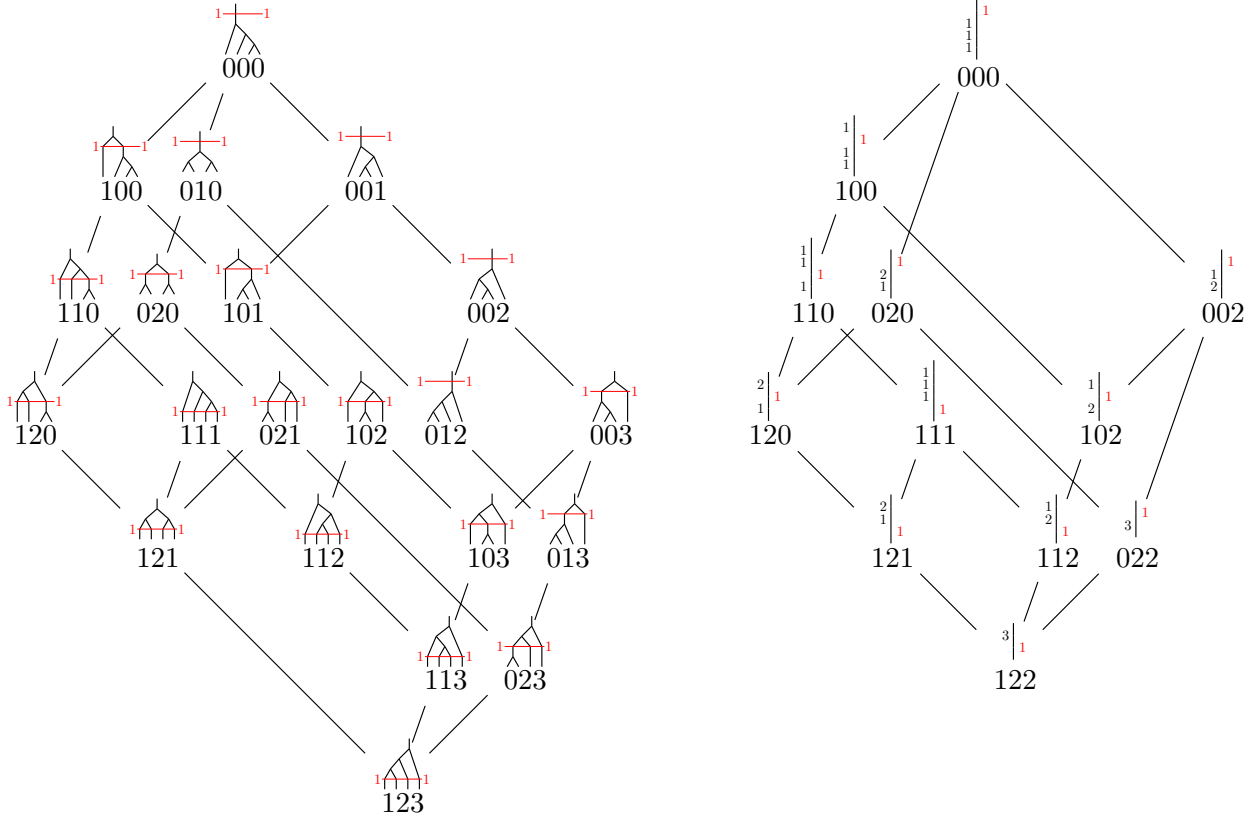
FIGURE 21. Cubic realizations of the 1-painted 3-tree (left) and 1-lighted 3-shade (right) rotation lattices.

3.2. **Cubic (m, n)-multiplihedron.** We now briefly present the cubic realizations of the m-painted n-tree refinement poset and rotation lattice. These are a mixture of the Lehmer codes of the permutations of $[m]$ and the bracket vectors of the binary trees with n nodes. The case $m = 1$ was already discussed in [SU04, above Figure 11]. It is convenient to use the poset $\prec_{\mathbb{T}}$ to define the cubic vector of

Definition 72. The *cubic vector* of a binary m-painted n-tree $\mathbb{T}$ is the vector $\boldsymbol{C}(\mathbb{T}) := \big(C_j(\mathbb{T})\big)_{j \in [m+n]}$ where $C_j(\mathbb{T}) := \#\{i < j \mid i \prec_{\mathbb{T}} j\}$. Note that $C_j(\mathbb{T}) \in \{0, \dots, j-1\}$, so that it is standard to forget the first coordinate (which is always 0).

Example 73. Observe that

- when $n = 0$, we have the Lehmer code of a permutation presented in Example 70,
- when $m = 0$, we have the bracket vector of a binary tree presented in Example 71.

The following statement is illustrated in Figures 21 to 23 (top). We skip its proof as it is a straightforward generalization of the permutahedron and associahedron cases.

Proposition 74. *The cubic vectors of m-painted n-trees define*

- *a cubic realization of the right rotation lattice on m-painted n-trees,*
- *a cubic subdivision realizing the face lattice of the (m, n)-multiplihedron $\mathbb{M}ul(m, n)$ by the set of cubes $\mathrm{Cube}\big(\boldsymbol{C}(\mathbb{T}), \boldsymbol{C}(\mathbb{T}')\big)$ for $\mathbb{T} \leq \mathbb{T}'$ defining a face of $\mathbb{M}ul(m, n)$.*

FIGURE 22. Cubic realizations of the m-painted n-tree rotation lattice (top) and the m-lighted n-shade rotation lattice (bottom) for $(m, n) = (0, 3)$, $(1, 2)$, $(2, 1)$, and $(3, 0)$ (left to right).

FIGURE 23. Cubic realizations of the m-painted n-tree rotation lattice (top) and the m-lighted n-shade rotation lattice (bottom) for $(m, n) = (0, 4)$, $(1, 3)$, $(2, 2)$, $(3, 1)$, and $(4, 0)$ (left to right).

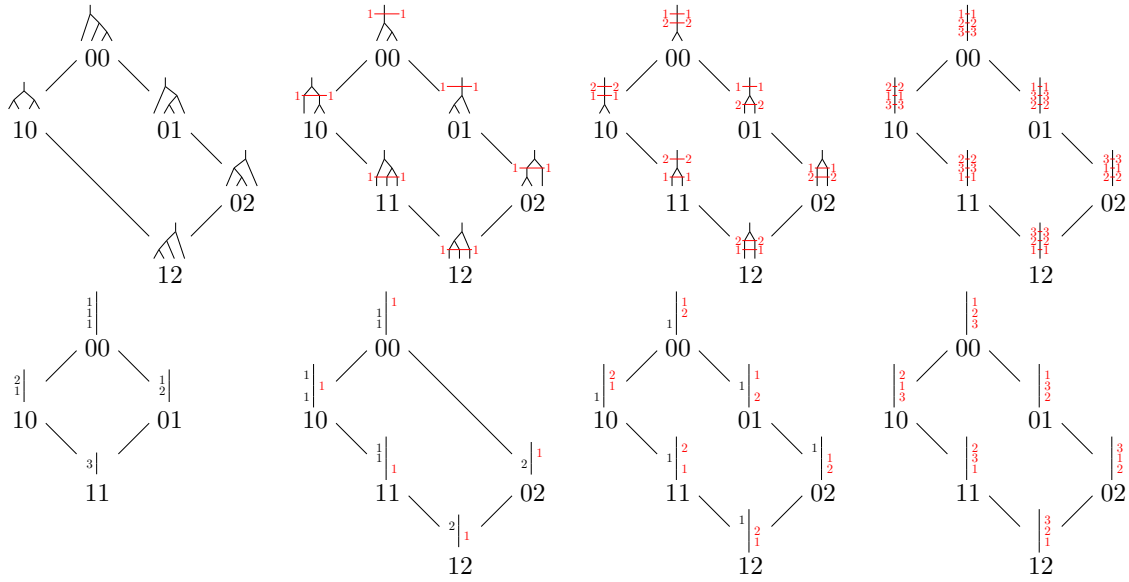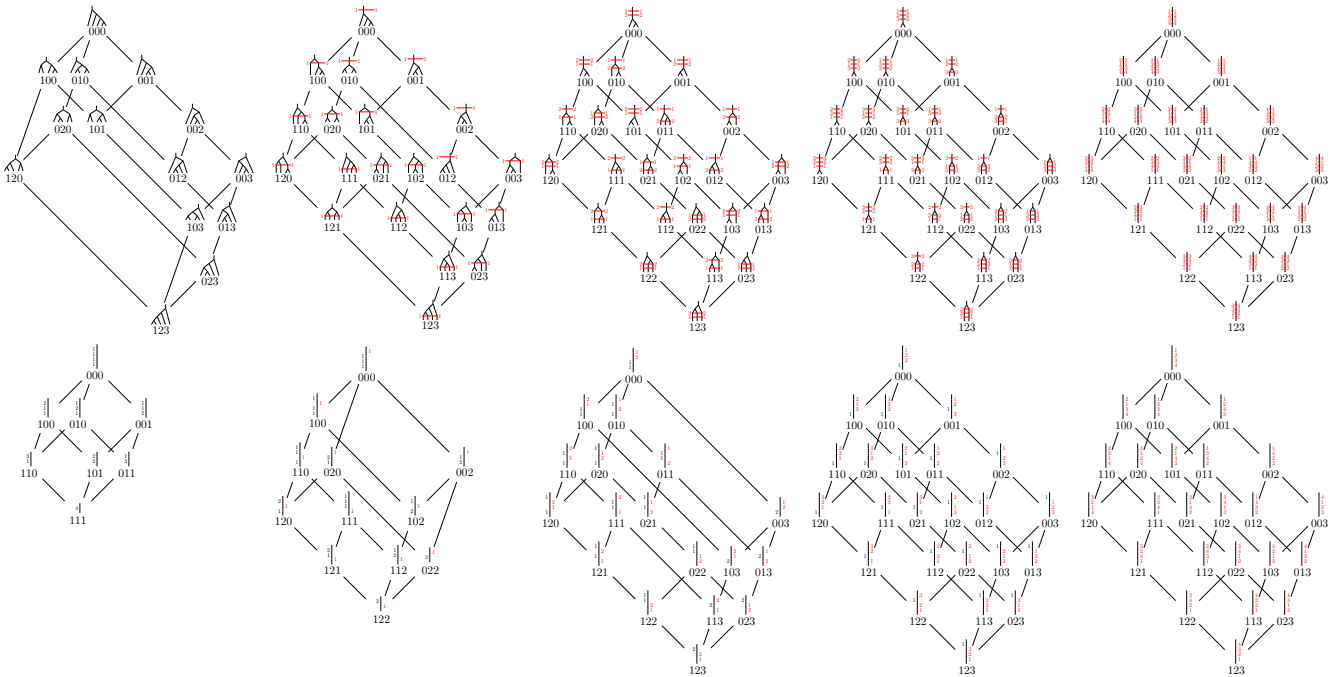3.3. **Cubic (m,n)-Hochschild polytope.** We now provide cubic realizations for the (m,n)-Hochschild polytope. Unfortunately, the formula for the cubic coordinates of an m-lighted n-shade $\mathbb{S}$ is not just obtained by counting non-inversions in $\prec_{\mathbb{S}}$ (*i.e.* pairs $i < j$ with $i \prec_{\mathbb{S}} j$). We thus first introduce a bijection between the m-lighted n-shades and the (m,n)-Hochschild words, generalizing the triwords of [San09, RS18, Cha20, Com21, Müh22]. We then use these (m,n)-Hochschild words to obtain cubic realizations.

3.3.1. (m,n)-*Hochschild words.* We start with (m,n)-words, defined as follows.

Definition 75. A (m,n)-word is a word $w := w_1 \ldots w_n$ of length n on the alphabet $\{0, 1, ..., m+1\}$ such that

- $w_1 \neq m+1$
- for $s \in [1,m]$, $w_i = s$ implies $w_j \geq s$ for all $j < i$

We denote by $W(m,n)$ the poset of (m,n)-words ordered componentwise (*i.e.* $w \leq w'$ if and only if $w_i \leq w_i'$ for all $i \in [n]$).

Example 76. When $m = 0$, the second condition is empty, so that the $(0,n)$-words are binary words of length n starting with a 0, and $W(0,n)$ is isomorphic to the boolean lattice on $n-1$ letters. When $m = 1$, the $(1,n)$-words are precisely the triwords of [San09, RS18, Cha20, Com21, Müh22], and $W(1,n)$ is isomorphic to the Hochschild lattice.

Definition 77. A (m,n)-Hochschild word is a pair of (σ, w) where σ is a permutation of $[m]$ and w is an (m,n)-word.

We now define a bijection between the m-lighted n-shades and the (m,n)-Hochschild words. Recall that we denote by $ps(x)$ the preceeding sum of an entry x in an m-lighted n-shade (see Definition 19).

Definition 78. Consider a unary m-lighted n-shade $\mathbb{S} := (S, C, \sigma)$ and denote by $s_1, \ldots, s_k$ of values of the singleton tuples of S. We associate to $\mathbb{S}$ an (m,n)-Hochschild word (σ, w), where the permutation is the permutation σ of the labels of the cuts of $\mathbb{S}$, and the (m,n)-word w has pth entry w_p given by

- if there is $j \in [k]$ such that $p = ps(s_j) - m - s_j + 1$, then the number of cuts below s_j,
- $m + 1$ otherwise.

In other words, for each s_j, we write the number of cuts below s_j followed by $s_j - 1$ copies of $m+1$. See Figures 24 and 25 for some examples.

Definition 79. Conversely, we associate to an (m,n)-Hochschild word (σ, w) a unary m-lighted n-shade $\mathbb{S} := (S, C, \sigma)$ where the labels of the cuts of $\mathbb{S}$ is given by the permutation σ, and the n-shade S is the sequence of (either singleton or empty) tuples

$$S := (s_{m,1}) \ldots (s_{m,k_m})(\varnothing) \ldots (\varnothing)(s_{i,1}) \ldots (s_{i,k_i})(\varnothing) \cdots (\varnothing)(s_{0,1}) \ldots (s_{0,k_0}),$$

where the $s_{i,j} \geq 1$ are such that

$$w = m(m+1)^{s_{m,1}-1} \ldots i(m+1)^{s_{1,k_i}-1} \ldots i(m+1)^{s_{i,k_i}-1} \ldots 0(m+1)^{s_{0,k_0}-1}.$$

In other words, we place the m cuts-to-be, and place a tuple (s) before the $(m - i + 1)$st cut for each maximal subword of w of the form $i(m+1)^{s-1}$. See Figures 24 and 25 for some examples.

Lemma 80. *The maps of Definitions 78 and 79 are inverse bijections between the unary m-lighted n-shades and the (m,n)-Hochschild words.*

Proof. First, the word associated to a unary m-lighted n-shade is an (m,n)-word. Indeed,

- the first letter is not $m+1$, because there are only m cuts,
- as we are reading the shade from top to bottom, the numbers written before the number $s \in [1,m]$ come from higher entries that have at least s cuts below them, so these numbers are at least s.
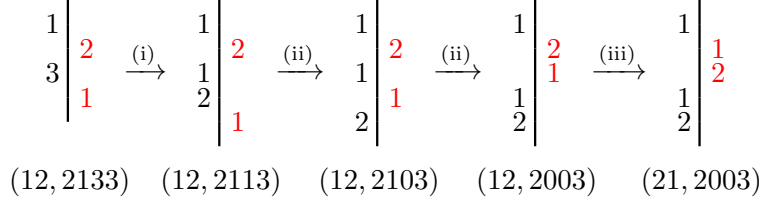
$$\left.\begin{matrix} 1 \\ \color{red}2 \\ 3 \quad \color{red}1 \end{matrix}\right| \xrightarrow{\text{(i)}} \left.\begin{matrix} 1 \\ \color{red}2 \\ 1 \\ 2 \quad \color{red}1 \end{matrix}\right| \xrightarrow{\text{(ii)}} \left.\begin{matrix} 1 \\ \color{red}2 \\ 1 \\ 2 \quad \color{red}1 \end{matrix}\right| \xrightarrow{\text{(ii)}} \left.\begin{matrix} 1 \\ \color{red}2 \\ \color{red}1 \\ 2 \end{matrix}\right| \xrightarrow{\text{(iii)}} \left.\begin{matrix} 1 \\ \color{red}1 \\ \color{red}2 \\ 2 \end{matrix}\right|$$

$$(12, 2133) \quad (12, 2113) \quad (12, 2103) \quad (12, 2003) \quad (21, 2003)$$

FIGURE 24. Some unary 2-lighted 4-shades and their $(2, 4)$-Hochschild words.

$$\left.\begin{matrix} 3 \\ \quad \color{red}1 \end{matrix}\right| \left.\begin{matrix} 2 \\ 1 \\ \quad \color{red}1 \end{matrix}\right| \left.\begin{matrix} 1 \\ 2 \\ \quad \color{red}1 \end{matrix}\right| \left.\begin{matrix} 2 \\ 1 \quad \color{red}1 \end{matrix}\right| \left.\begin{matrix} 1 \\ 1 \\ 1 \\ \quad \color{red}1 \end{matrix}\right| \left.\begin{matrix} 1 \\ 3 \quad \color{red}1 \end{matrix}\right| \left.\begin{matrix} 1 \\ 1 \\ \quad \color{red}1 \end{matrix}\right| \left.\begin{matrix} 1 \\ 2 \quad \color{red}1 \end{matrix}\right| \left.\begin{matrix} 1 \\ 1 \quad \color{red}1 \end{matrix}\right| \left.\begin{matrix} 2 \\ 1 \quad \color{red}1 \end{matrix}\right| \left.\begin{matrix} 1 \\ 2 \quad \color{red}1 \end{matrix}\right| \left.\begin{matrix} 1 \\ 1 \\ 1 \quad \color{red}1 \end{matrix}\right|$$

$$(1, 122) \ (1, 121) \ (1, 112) \ (1, 120) \ (1, 111) \ (1, 022) \ (1, 110) \ (1, 102) \ (1, 100) \ (1, 020) \ (1, 002) \ (1, 000)$$
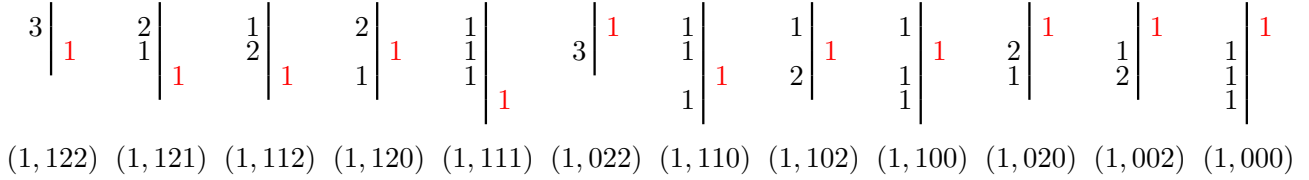
FIGURE 25. All unary 1-lighted 3-shades and $(1, 3)$-Hochschild words.

Conversely, the sequence of tuples associated to an (m, n)-Hochschild word is a unary m-lighted n-shade. Indeed, the total sum is the length of w, and each tuple is either empty or a singleton contained in a singleton cut.

Finally, it is immediate to check that the two maps are inverse to each other. $\qquad\square$

Remark 81. Through the bijection of Definition 78, we can thus transport the rotation lattice on unary m-lighted n-shades to a lattice on (m, n)-Hochschild words. The relation between (m, n)-Hochschild words can be described as follows. For two Hochschild words (σ, v) and (τ, w), we have $(\sigma, v) \leq (\tau, w)$, if

- $\sigma \leq \tau$ in weak order,
- $v \leq w$ coordinatewise,
- there exists a reduced expression $\sigma^{-1} \circ \tau = \tau_{i_1} \circ \ldots \circ \tau_{i_k}$ (*i.e.* a path in the permutahedron from σ to τ) and a sequence of (m, n)-words $v = h_0 \leq h_1 \leq h_2 \ldots \leq h_k = w$ such that h_l does not have the entry i_l.

The lattice is thus a subposet in the Cartesian product between the weak order on permutations of $[m]$ and the (m, n)-word poset $W(m, n)$. It would be nice to have a more explicit formulation of the last condition in the descriprion of the relation $(\sigma, v) \leq (\tau, w)$, but we were not able to find it.

Finally, as it is a fiber of the lattice morphism $(\sigma, w) \mapsto \sigma$ from the (m, n)-Hochschild word rotation lattice to the weak order, we obtain that the (m, n)-word poset $W(m, n)$ is a lattice. As mentioned in Remark 29, it seems to have much more interesting properties than the (m, n)-Hochschild word rotation lattice (for instance, it seems to be extremal, and its Coxeter polynomial seems to be a product of cyclotomic polynomials).

Corollary 82. *The (m, n)-word poset $W(m, n)$ is a lattice.*

Remark 83. The lattice $W(1, n)$ has a geometric interpretation in the context of homotopical algebra. Specifically, the Hochschild polytope $\mathbb{H}och(1, n)$ has a polytopal subdivision whose directed 1-skeleton is $W(m, n)$. The Hochschild polytopes $\mathbb{H}och(1, n)$ form an operadic bimodule over the operad of skew cubes $\mathbb{H}och(0, n)$ in the category of CW-spaces [Pol20], and tensor powers of this bimodule over the operad are CW-isomorphic to this subdivision. Algebraically this allows for the composition of sequences of morphisms of A_∞-modules over DG-algebras (or of representations up to homotopy [ACD11]).

3.3.2. *Cubic realizations.* Passing from the unary m-lighted n-shades to the (m,n)-Hochschild words allows us to construct cubic realizations for the m-lighted n-shade refinement lattice and rotation lattice.

Definition 84. The *cubic vector* of an (m,n)-Hochschild word is the vector obtained by the concatenation of the Lehmer code of σ (forgetting the first coordinates which is always 0) with the (m,n)-word w. The *cubic vector* $\boldsymbol{C}(\mathbb{S})$ of a unary m-lighted n-shade $\mathbb{S}$ is the cubic vector of the associated (m,n)-Hochschild word via the bijection of Definition 78.

The following statement is illustrated in Figures 21 to 23 (top).

Proposition 85. *The cubic vectors of m-lighted n-shades define*
- *a cubic realization of the right rotation lattice on m-lighted n-shades,*
- *a cubic subdivision realizing the face lattice of the (m,n)-Hochschild polytope $\mathbb{Hoch}(m,n)$ by the set of cubes $\mathrm{Cube}\big(\boldsymbol{C}(\mathbb{S}), \boldsymbol{C}(\mathbb{S}')\big)$ for $\mathbb{S} \leq \mathbb{S}'$ defining a face of $\mathbb{Hoch}(m,n)$.*

Proof. We proceed by induction, starting from the Lehmer–Saneblidze–Umble realization of permutahedra for the case $\mathbb{Hoch}(m,0)$. Suppose that the cubic subdivision for $\mathbb{Hoch}(m,n-1)$ is already constructed. To obtain the cubic subdivision of $\mathbb{Hoch}(m,n)$, we further subdivide the boundary of $\mathbb{Hoch}(m,n-1) \times [0,n]$.

Let $\mathbb{S} := (S, C, \mu)$ be a shade corresponding to a d-dimensional face in $\mathbb{Hoch}(m,n-1)$, which can also be viewed as a subcube. For a cut $c_i \in C$ below all of S, let p_i represent the total size of all μ-parts on c_i and all the cuts below. The subdivision of $[0,n]$ relative to $\mathbb{S}$ is denoted by $[0,n]_{\mathbb{S}}$, and it consists of the subdivision of $[0,n]$ by the points p_i. The intervals in $[0,n]_{\mathbb{S}}$ correspond to the $(d+1)$-dimensional shades that map to $\mathbb{S}$ under the "forgetting the last leaf" map. Refinement of shades corresponds to refinement of relative interval subdivisions. Then $\mathbb{Hoch}(m,n-1) \times [0,n]$ subdivides as $\bigcup_{\mathbb{S}} \mathbb{S} \times [0,n]_{\mathbb{S}}$. The vertex coordinates coincide with the construction above, by description of points p_i for unary $\mathbb{S}$ where each cut carries a μ-part of size 1. □

Remark 86. This cubic realization provides an alternative proof of the lattice property, using induction and the fact that fibers of the map $\pi : \mathrm{Hoch}(m,n) \to \mathrm{Hoch}(m,n-1)$ are totally ordered. Indeed, assuming that $\mathrm{Hoch}(m,n-1)$ is known to be a lattice, let $\mathbb{S}$ and $\mathbb{S}'$ be two elements in $\mathrm{Hoch}(m,n)$ whose meet we want to find. Observe that the point with coordinates $(\pi(\mathbb{S}) \wedge \pi(\mathbb{S}'), 0)$ is smaller than both $\mathbb{S}$ and $\mathbb{S}'$. The meet of $\mathbb{S}$ and $\mathbb{S}'$ is thus the largest element in the fiber of $\pi(\mathbb{S}) \wedge \pi(\mathbb{S})$ which is smaller than both $\mathbb{S}$ and $\mathbb{S}'$ (it exists as the fiber is totally ordered).

References

[ABD10] Federico Ardila, Carolina Benedetti, and Jeffrey Doker. Matroid polytopes and their volumes. *Discrete Comput. Geom.*, 43(4):841–854, 2010.

[ACD11] Camilo Arias Abad, Marius Crainic, and Benoit Dherin. Tensor products of representations up to homotopy. *Journal of Homotopy and Related Structures*, 6(2):239–288, 2011.

[AD13] Federico Ardila and Jeffrey Doker. Lifted generalized permutahedra and composition polynomials. *Adv. in Appl. Math.*, 50(4):607–633, 2013.

[Cha20] Frédéric Chapoton. Some properties of a new partial order on Dyck paths. *Algebr. Comb.*, 3(2):433–463, 2020.

[Cha23] Frédéric Chapoton. Posets and Fractional Calabi-Yau Categories. Preprint, arXiv:2303.11656 , 2023.

[Com21] Camille Combe. A geometric and combinatorial exploration of Hochschild lattices. *Electron. J. Combin.*, 28(2):Paper No. 2.38, 29, 2021. With an appendix by Frédéric Chapoton.

[CP17] Grégory Chatel and Vincent Pilaud. Cambrian Hopf Algebras. *Adv. Math.*, 311:598–633, 2017.

[CP22] Frédéric Chapoton and Vincent Pilaud. Shuffles of deformed permutahedra, multiplihedra, constrainahedra, and biassociahedra. Preprint, arXiv:2201.06896, 2022.

[Edm70]   Jack Edmonds. Submodular functions, matroids, and certain polyhedra. In *Combinatorial Structures and their Applications*, pages 69–87. Gordon and Breach, New York, 1970.

[FLS10]   Stefan Forcey, Aaron Lauve, and Frank Sottile. Hopf structures on the multiplihedra. *SIAM J. Discrete Math.*, 24(4):1250–1271, 2010.

[For08]   Stefan Forcey. Convex hull realizations of the multiplihedra. *Topology Appl.*, 156(2):326–347, 2008.

[FZ02]   Sergey Fomin and Andrei Zelevinsky. Cluster algebras. I. Foundations. *J. Amer. Math. Soc.*, 15(2):497–529, 2002.

[FZ03]   Sergey Fomin and Andrei Zelevinsky. Cluster algebras. II. Finite type classification. *Invent. Math.*, 154(1):63–121, 2003.

[HLT11]   Christophe Hohlweg, Carsten Lange, and Hugh Thomas. Permutahedra and generalized associahedra. *Adv. Math.*, 226(1):608–640, 2011.

[HNT05]   Florent Hivert, Jean-Christophe Novelli, and Jean-Yves Thibon. The algebra of binary search trees. *Theoret. Comput. Sci.*, 339(1):129–165, 2005.

[HPS18]   Christophe Hohlweg, Vincent Pilaud, and Salvatore Stella. Polytopal realizations of finite type **g**-vector fans. *Adv. Math.*, 328:713–749, 2018.

[HT72]   Samuel Huang and Dov Tamari. Problems of associativity: A simple proof for the lattice property of systems ordered by a semi-associative law. *J. Combinatorial Theory Ser. A*, 13:7–13, 1972.

[Lan13]   Carsten E. M. C. Lange. Minkowski decomposition of associahedra and related combinatorics. *Discrete Comput. Geom.*, 50(4):903–939, 2013.

[Leh60]   Derrick Henry Lehmer. Teaching combinatorial tricks to a computer. In *Proc. Sympos. Appl. Math., Vol. 10*, pages 179–193. American Mathematical Society, Providence, R.I., 1960.

[Lod04]   Jean-Louis Loday. Realization of the Stasheff polytope. *Arch. Math. (Basel)*, 83(3):267–278, 2004.

[LR98]   Jean-Louis Loday and María O. Ronco. Hopf algebra of the planar binary trees. *Adv. Math.*, 139(2):293–309, 1998.

[MR95]   Claudia Malvenuto and Christophe Reutenauer. Duality between quasi-symmetric functions and the Solomon descent algebra. *J. Algebra*, 177(3):967–982, 1995.

[Müh22]   Henri Mühle. Hochschild lattices and shuffle lattices. *European J. Combin.*, 103:Paper No. 103521, 31, 2022.

[MW10]   S. Ma'u and C. Woodward. Geometric realizations of the multiplihedra. *Compos. Math.*, 146(4):1002–1028, 2010.

[OEIS]   The On-Line Encyclopedia of Integer Sequences. Published electronically at http://oeis.org, 2010.

[Pil18]   Vincent Pilaud. Brick polytopes, lattice quotients, and Hopf algebras. *J. Combin. Theory Ser. A*, 155:418–457, 2018.

[Pil19]   Vincent Pilaud. Hopf algebras on decorated noncrossing arc diagrams. *J. Combin. Theory Ser. A*, 161:486–507, 2019.

[Pol20]   Daria Poliakova. Cellular chains on freehedra and operadic pairs. Preprint, arXiv:2011.11607, 2020.

[Pos09]   Alexander Postnikov. Permutohedra, associahedra, and beyond. *Int. Math. Res. Not. IMRN*, (6):1026–1106, 2009.

[PP18]   Vincent Pilaud and Viviane Pons. Permutrees. *Algebraic Combinatorics*, 1(2):173–224, 2018.

[PRW08]   Alexander Postnikov, Victor Reiner, and Lauren K. Williams. Faces of generalized permutohedra. *Doc. Math.*, 13:207–273, 2008.

[PS19]   Vincent Pilaud and Francisco Santos. Quotientopes. *Bull. Lond. Math. Soc.*, 51(3):406–420, 2019.

[PSZ23]   Vincent Pilaud, Francisco Santos, and Günter M. Ziegler. Celebrating loday's associahedron. Preprint, arXiv:2305.08471, 2023.

[Rad52]   Richard Rado. An inequality. *J. London Math. Soc.*, 27:1–6, 1952.

[Rea05]   Nathan Reading. Lattice congruences, fans and Hopf algebras. *J. Combin. Theory Ser. A*, 110(2):237–273, 2005.

[Rea06]   Nathan Reading. Cambrian lattices. *Adv. Math.*, 205(2):313–353, 2006.

[RS09]   Nathan Reading and David E. Speyer. Cambrian fans. *J. Eur. Math. Soc.*, 11(2):407–447, 2009.

[RS18]   Manuel Rivera and Samson Saneblidze. A combinatorial model for the free loop fibration. *Bull. Lond. Math. Soc.*, 50(6):1085–1101, 2018.

[San09]   Samson Saneblidze. The bitwisted Cartesian model for the free loop fibration. *Topology Appl.*, 156(5):897–910, 2009.

[Sch11]   Pieter Hendrik Schoute. *Analytical treatment of the polytopes regularly derived from the regular polytopes. Section I: The simplex.*, volume 11. 1911.

[SS93]   Steve Shnider and Shlomo Sternberg. *Quantum groups: From coalgebras to Drinfeld algebras*. Series in Mathematical Physics. International Press, Cambridge, MA, 1993.

[Sta63]   Jim Stasheff. Homotopy associativity of H-spaces I & II. *Trans. Amer. Math. Soc.*, 108(2):275–312, 1963.

[SU04]   Samson Saneblidze and Ronald Umble. Diagonals on the permutahedra, multiplihedra and associahedra. *Homology Homotopy Appl.*, 6(1):363–411, 2004.

[Tam51]   Dov Tamari. *Monoides préordonnés et chaînes de Malcev*. PhD thesis, Université Paris Sorbonne, 1951.

[Ton97]   Andy Tonks. Relating the associahedron and the permutohedron. In *Operads: Proceedings of Renaissance Conferences (Hartford, CT/Luminy, 1995)*, volume 202 of *Contemp. Math.*, pages 33–36. Amer. Math. Soc., Providence, RI, 1997.

Appendix A. Enumeration tables

All references like A000142 are entries of the Online Encyclopedia of Integer Sequences [OEIS].

A.1. **Multiplihedra.**

$m\backslash n$	0	1	2	3	4	5	6	7	8	9	
0	.	1	2	5	14	42	132	429	1430	4862	A000108
1	1	2	6	21	80	322	1348	5814	25674		A121988
2	2	6	24	108	520	2620	13648	72956			$2 \cdot$ A158826
3	6	24	120	660	3840	23220	144504				?
4	24	120	720	4680	31920	225120					
5	120	720	5040	37800	295680						
6	720	5040	40320	342720							
7	5040	40320	362880								
8	40320	362880									
9	362880										
	A000142	A000142	A000142	A084253	?						$m! \cdot$ A158825

Table 1. Number of vertices of the multiplihedra $\mathbb{M}ul(m,n)$. See A158825.

$m\backslash n$	0	1	2	3	4	5	6	7	8	9	
0	.	1	2	5	9	14	20	27	35	44	A000096
1	1	2	6	13	25	46	84	155	291		A335439
2	2	6	14	29	57	110	212	411			?
3	6	14	30	61	121	238	468				
4	14	30	62	125	249	494					
5	30	62	126	253	505						
6	62	126	254	509							
7	126	254	510								
8	254	510									
9	510										
	A000918	A000918	A000918	A036563	A048490	?					

Table 2. Number of facets of the multiplihedra $\mathbb{M}ul(m,n)$.

$m\backslash n$	0	1	2	3	4	5	6	7	8	9	
0	.	1	3	11	45	197	903	4279	20793	103049	A001003
1	1	3	13	67	381	2311	14681	96583	653049		?
2	3	13	75	497	3583	27393	218871	1810373			
3	13	75	541	4375	38073	349423	3341753				
4	75	541	4683	44681	454855	4859697					
5	541	4683	47293	519847	6055401						
6	4683	47293	545835	6790697							
7	47293	545835	7087261								
8	545835	7087261									
9	7087261										
	A000670	A000670	A000670	?							

Table 3. Total number of faces of the multiplihedra $\mathbb{M}ul(m,n)$. The empty face is not counted, but the polytope itself is.

A.2. **Hochschild polytopes.**

$m\backslash n$	0	1	2	3	4	5	6	7	8	9	
0	.	1	2	4	8	16	32	64	128	256	A000079
1	2	2	5	12	28	64	144	320	704		A045623
2	6	6	18	50	132	336	832	2016			?
3	24	24	84	264	774	2160	5808				
4	120	120	480	1680	5400	16344					
5	720	720	3240	12480	43560						
6	5040	5040	25200	105840							
7	40320	40320	221760								
8	362880	362880									
9	3628800										
	A000142	A000142	A038720	?							

TABLE 4. Number of vertices of the Hochschild polytope $\mathbb{H}\text{och}(m, n)$. See A158825.

$m\backslash n$	0	1	2	3	4	5	6	7	8	9	
0	.	0	2	4	6	8	10	12	14	16	A005843
1	0	2	5	8	11	14	17	20	23		A016789
2	2	6	11	16	21	26	31	36			A016861
3	6	14	23	32	41	50	59				A017221
4	14	30	47	64	81	98					?
5	30	62	95	128	161						
6	62	126	191	256							
7	126	254	383								
8	254	510									
9	510										
	A000918	A000918	A055010	A000079	A083575	A164094	A164285	A140504	?		

TABLE 5. Number of facets of the Hochschild polytope $\mathbb{H}\text{och}(m, n)$.

$m\backslash n$	0	1	2	3	4	5	6	7	8	9	
0	.	1	3	9	27	81	243	729	2187	6561	A000244
1	1	3	11	39	135	459	1539	5103	16767		?
2	3	13	57	233	909	3429	12609	45441			
3	13	75	383	1767	7635	31491	125415				
4	75	541	3153	16169	76437	341205					
5	541	4683	30671	172839	885795						
6	4683	47293	343857	2110313							
7	47293	545835	4362383								
8	545835	7087261									
9	7087261										
	A000670	A000670	?								

TABLE 6. Total number of faces of the Hochschild polytope $\mathbb{H}\text{och}(m, n)$. The empty face is not counted, but the polytope itself is.

A.3. **Singletons.**

$m\backslash n$	0	1	2	3	4	5	6	7	8	9	
0	.	1	2	3	5	8	13	21	34	55	A000045
1	1	2	4	7	12	20	33	54	88		A000071
2	2	6	14	28	52	92	158	266			?
3	6	24	66	150	306	582	1056				
4	24	120	384	984	2208	4536					
5	120	720	2640	7560	18600						
6	720	5040	20880	66240							
7	5040	40320	186480								
8	40320	362880									
9	362880										
	A000142	A000142	?								

TABLE 7. Number of shadow singletons, *i.e.* common vertices of the (m,n)-multiplihedron $\mathbb{Mul}(m,n)$ and the (m,n)-Hochschild polytope $\mathbb{Hoch}(m,n)$.

CNRS & LIX, École Polytechnique, Palaiseau
Email address: vincent.pilaud@lix.polytechnique.fr
URL: http://www.lix.polytechnique.fr/~pilaud/

University of Southern Denmark, Odense
Email address: polydarya@gmail.com